17434

NATIONAL LIBRARY
OTTAWA

CANADA

BIBLIOTHÈQUE NATIONALE
OTTAWA

NAME OF AUTHOR.. ARI ARNALDS

TITLE OF THESIS... An Optical Matched Filter generated by a Computer

UNIVERSITY... U. of ALBERTA

DEGREE FOR WHICH THESIS WAS PRESENTED... M.Sc.

YEAR THIS DEGREE GRANTED... 1973

Permission is hereby granted to THE NATIONAL LIBRARY OF CANADA to microfilm this thesis and to lend or sell copies of the film.

The author reserves other publication rights, and neither the thesis nor extensive extracts from it may be printed or otherwise reproduced without the author's written permission.

(Signed) Ari Arnalds

PERMANENT ADDRESS:

BARMAHLID 13

REYKJAVIK

ICELAND

DATED... ~~10/3~~ 24/10 ... 1973
A.A.

NL-91 (10-68)

THE UNIVERSITY OF ALBERTA

AN OPTICAL MATCHED FILTER GENERATED BY A COMPUTER

by

© ARI ARNALDS

SUBMITTED TO THE FACULTY OF GRADUATE STUDIES AND RESEARCH
IN PARTIAL FULFILMENT OF THE REQUIREMENTS FOR THE DEGREE
OF MASTER OF SCIENCE
IN
ELECTRICAL ENGINEERING

DEPARTMENT OF ELECTRICAL ENGINEERING

EDMONTON, ALBERTA

FALL 1973

THE UNIVERSITY OF ALBERTA

FACULTY OF GRADUTE STUDIES AND RESEARCH

The undersigned certify that they have read, and recommend to the Faculty of Graduate Studies and Research, for acceptance, a thesis entitled "An Optical Matched Filter Generated by a Computer", submitted by Ari Arnalds in partial fulfilment of the requirements for the degree of Master of Science, in Electrical Engineering.

H. G. Lehmann
Supervisor

W. A. Davis

Keith Hagmaier

A. Regier

Date Oct. 18th 1973

ABSTRACT

This thesis is concerned with the use of computer generated binary masks, invented by A. W. Lohman, as matched filters.

A theoretical analysis of the transmission properties of a filter previously invented by A. B. Vander Lught is presented and it is shown that the Lohman filter can be regarded as a binary simulation of a Vander Lught filter.

Using fingerprints as test objects, the computational requirements for the evaluation of parameters describing a Lohman filter are examined and the production of a filter is explained in detail.

Several Lohman filters designed to detect fingerprints are made and experimentally tested. The experimental results demonstrate the ability of a Lohman mask to identify fingerprints and show that the accuracy achievable with the experimental system used in the present work permits 49 prints to be processed in parallel.

ACKNOWLEDGEMENTS

The author wishes to thank his supervisor, Dr. H. G. Schmidt-Weinmar, for leading him to the topic of this thesis. The advice given by Dr. H. G. Schmidt-Weinmar during the preparation of the thesis is also acknowledged.

The author is also indebted to Dr. H. J. Seguin for his advice and loan of most of the equipment used in the experiments described in this thesis.

Appreciation is also extended to Dr. W. A. Davis and other members of the Department of Computing Science for the use of the image conversion system, and their assistance in its use.

Last but not least, I thank my wife, Sigrun, for her patience and encouragement during this work. Sigrun also drew all the figures in this thesis and helped in many other ways in its production.

The financial assistance recieved from the Department of Electrical Engineering, the National Research Council and the Faculty of Graduate Studies and Research is also gratefully acknowledged.

TABLE OF CONTENTS

		Page
CHAPTER 1	INTRODUCTION	1
1.1	Spatial Filtering	1
1.2	Vander Lught vs. Lohman Filters	5
1.3	Scope of the Thesis	6
CHAPTER 2	THEORETICAL BACKGROUND	9
2.1	The Fourier Transform	9
2.2	Linear Systems	10
2.3	Space-Invariant Linear Systems	12
2.4	Fourier Transformation by Lenses Optical Filtering System	13
2.5	The Matched Filter	17
2.6	Production of Matched Filters	21
CHAPTER 3	VANDER LUGHT AND LOHMAN FILTERS	22
3.1	The Vander Lught Filter	22
3.2	The Lohman Filter	27
3.3	The Relationship between Vander Lught and Lohman Filters	35
3.4	Discussion	45
CHAPTER 4	SAMPLING CONSIDERATIONS	49
4.1	Introduction	49
4.2	Sampling Theorem - Aliasing	51

4.3 Frequency Bandlimitations of Fingerprints 56

CHAPTER 5 PRODUCTION OF A LOHMAN FILTER 62

5.1 Data Collection 62

5.2 Computing and Plotting 64

5.3 Cost of a Filter 66

CHAPTER 6 EXPERIMENTS 68

6.1 Experimental Arrangement 68

6.2 Positioning Accuracy Required 71

6.3 Experimental Equipment 73

6.4 Experimental Results 77

6.5 Discussion 86

CHAPTER 7 SUMMARY AND CONCLUSIONS 91

REFERENCES 96

APPENDIX A DERIVATION OF EQUATION (3.12) 98

APPENDIX B COMPUTER PROGRAMS 101

LIST OF TABLES

Page

Table 1. Results of fingerprint recognition experiment. Filter matched to object no. 1. 80

Table 2. Results of fingerprint recognition experiment. Filter matched to object no. 2. 81

Table 3. Results of fingerprint recognition experiment. Filter matched to object no. 3. 82

LIST OF FIGURES

		Page
Figure 1.	Optical filtering system.	15
Figure 2.	Optical system defining a matched filter.	20
Figure 3.	Optical system to record a Vander Lught filter	23
Figure 4.	A cell of a Lohman filter.	29
Figure 5.	Matched filter illuminated by a plane wave.	30
Figure 6.	Plot of the real part of the reference wave distribution as a function of x_n.	39
Figure 7.	The transmission function of a cell in the approximation to a Vander Lught filter.	42
Figure 8.	Modified transmission function of a cell in the approximation to a Vander Lught filter.	44
Figure 9.	Approximations to a transmission function of a cell in a Vander Lught filter with $P_{nm}=G_{nm}=1/2$.	47
Figure 10.	The spectrum of a sampled signal.	54
Figure 11.	Computed Fourier transform of the letter A.	55
Figure 12.	Percentage of total power as a function of band-limit. Low-frequency print.	59
Figure 13.	Percentage of total power as a function of band-limit. High-frequency print.	60
Figure 14.	Production of a Lohman filter.	63
Figure 15.	Optical filtering system used for experimentation.	70
Figure 16.	Mechanical design to position filter in u direction.	75

Figure 17. Power in the recognition spot as a function of placement error perpendicular to optical axis. 84

Figure 18. Power in the recognition spot as a function of error in angular position. 85

CHAPTER 1

INTRODUCTION

1.1 Spatial Filtering

In recent years the interest in optical data processing, or optical computing as it has come to be called, has increased rapidly. Amongst the most successful branches of optical computing is the field of spatial filtering [1].

The meaning of spatial filtering will be explained later in some detail but at this moment it is sufficient to say that a spatial filter is a two-dimensional transparency or mask which in the most general case is required to control, in a predefined manner, the spatial distribution of both the amplitude and phase of a light wave passing through it. The attenuation of amplitude can be easily accomplished by the use of, for example, a darkened photographic plate. The control of the phase of a light wave was, however, a very difficult task until holographic techniques were developed.

The spatial filter considered in this thesis is a type of a matched filter. Historically, the matched filter was developed in electronic communication as the filter which maximizes the signal to noise ratio when detecting a signal submerged in white noise [2]. The usefulness of an optical matched filter is due to other reasons which follow.

The Fourier transform plays an important role in the theory of matched filtering. While the Fourier transformation of electric signals is a rather complicated operation, requiring extensive hardware, a single lens can perform the Fourier transformation on any optical signal, that is the two-dimensional distribution of magnitude and phase of the optical disturbance. It is this ability of a lens to readily perform a Fourier transformation which makes an optical matched filter an attractive tool regardless of the statistical distributions of the noise in which the signals to be detected are buried.

Prior to holographic techniques, spatial filters, including matched filters, were generally produced in two separate stages. The attenuation of amplitude was accomplished by the use of a darkened photographic plate and the control of phase was generally achieved by the use of a transparent film with appropriate variations in thickness. With these techniques it was only possible to implement rather simple transmission functions.

In 1963, A.B. Vander Lught invented a holcgraphic method of producing masks consisting only of an absorption pattern [3]. These masks therefore only affect the amplitude of light passing through them but nevertheless Vander Lught demonstrated that they could be used as matched filters despite the fact that they do not affect phase. This technique is therefore a method of reducing the

generally complex transmission function of a matched filter to a real transmission function.

The Vander Lught method was the first convenient method of prcducing optical matched filters and requires that the signal to be detected (the signal to which the filter is matched) is available in the form of a photographic transparency. This restricts the use of the Vander Lught technique tc real signals, that is signals which consist of amplitude distributions alone.

The Vander Lught filters have been applied to various signal detection problems including the recognition of alphanumeric characters [4] and fingerprint identification [5,6]. The experiments with fingerprint identification have shown particularly interesting results. These experiments show that despite the complexity of fingerprints they are detected with a high degree of accuracy by the Vander Lught filter. Even if only a fraction of a fingerprint is available to construct the filter, recognition is possible [5]. Also, the filter indicates similarity when the print to be recognized is superimposed by a second print [6]. In the last case the print to be detected was sc badly obscured by the superimposed print that it could not be identified by visual observation.

These properties of the Vander Lught filter are very important if they are to be used in criminal

investigations, since the prints collected at the scene of a crime are often incomplete or obscured by superimposed prints.

Systems have been developed which use the Vander Lught filter to identify a particular print from a file of a large number of prints [7]. In one experiment where such a system was used to identify 64 prints from a file of 10,000, in 65% of the cases the correct print only was identified and in 90% of the cases the system reduced the number of prints that had to be manually searched to less than 0.24% of the complete file.

In 1966, A.W. Lohman reported a method of producing optical filters (masks) consisting of only two different transmission levels [8]. These masks were originally intended for use as holograms but the inventors showed that they could also be used as matched filters.

This method of making matched filters uses a digital computer to evaluate parameters describing the required filter. The filter is then plotted by a computer-guided plotter in a greatly enlarged scale and finally this plot is photcgraphically reduced to the desired size.

Some of the applications which the Lohman mask has been used for are holography [9], code translation [10] and various filtering operations [11] including edge enhancement.

1.2 Vander Lught vs. Lohman Filters

The main advantage of a Vander Lught filter is that when the signal to be detected is available on a photographic transparency the filter is very easily produced. In the experiments mentioned previously the signals to be detected (letters and fingerprints) were available and the production of a Vander Lught filter was straightforward. For this reason rather limited attention has been paid to the Lohman masks as matched filters and no comprehensive study of their properties has been published.

In many respects, however, the Lohman filter has advantages over the Vander Lught filter. In order to produce a Lohman filter it is only necessary that the signal is known in mathematical terms. This is particularly important if the signal to be matched is not a real function but a complex one (i.e. the signal is both an amplitude and phase function). In this case a Lohman filter can easily be produced whereas the difficulty in obtaining the complex signal in the form of a transparency is considerable.

The situation described above, where it is desired to detect complex signals, frequently arises when optical components are to be tested [12].

If the signal to be detected is known to be submerged in noise, other than white noise, a filter which is optimum in the sense that it maximizes the signal to

noise ratio, can easily be made by the Lohman technique. All that is required is that the non-white noise distribution is allowed for when the filter is calculated. Such an optimum filter can also be produced by a modification of the Vander Lught technique [3] but the procedure is much more cumbersome than when the Lohman method is used.

It may be required to produce a filter matched to a signal which is not actually known but is to be found through experimentation or some sort of a learning process. In this case a Lohman filter could be synthesized directly whereas to synthesize a Vander Lught filter a signal would first have to be selected and realized.

The advantages of the Lohman filter described above only apply to its use as a matched filter, but it should be reiterated that the Lohman mask also has many other applications as indicated in the previous section.

There are therefore many instances where a Lohman mask is more suitable than a Vander Lught filter. For this reason it is desirable to investigate in some detail the performance of the Lohman filter and compare it to the Vander Lught filter.

1.3 Scope of the Thesis.

The scope of this thesis is to study the relationship between the two filters previously mentioned.

In Chapter 2 some theoretical background is given so that the content of the remaining chapters may be better understood. In Chapter 3 a detailed description is given of both the Lohman and Vander Lught filters and it is explained how a mask consisting only of an absorption pattern can act as a matched filter.

Also in Chapter 3 the relationship between the Vander Lught and Lohman filters is examined, and it will be shown that the transmission functions of the two filters are so similar that the Lohman filter can be regarded as a binary approximation to the Vander Lught filter.

When a Lohman filter is being produced, the signal must be sampled in order to enable the computing of the filter parameters. This leads to the question of how many samples are necessary to adequately represent the signal and what the computing costs involved are. This problem is considered in Chapter 4. As mentioned previously the results of experiments with fingerprints have shown promising results so all the experiments performed are done using fingerprints as test objects.

In Chapter 5 the various steps in the production of a Lohman filter, including the computation of the filter parameters and plotting of the filter, are explained in some detail and in Chapter 6 the results of fingerprint detection by Lohman filters are presented. The results of these experiments are compared with the published results of

similar experiments carried out with Vander Lught filters.

Finally, in Chapter 6 both theoretical and experimental results are summarized and discussed.

CHAPTER 2

THEORETICAL BACKGROUND

2.1 The Fourier Transform

As previously mentioned the Fourier transform is an important concept in the theory of spatial filtering.

If $g(x,y)$ is an optical signal in a plane with spatial coordinates (x,y) the Fourier transform of $g(x,y)$ is defined by

$$F\{g(x,y)\} = \int\int_{-\infty}^{\infty} g(x,y)\, \mathrm{Exp}[-j2\pi(ux+vy)]\,dxdy \qquad (2.1)$$

where $F\{\ \}$ denotes "Fourier transform of". A Fourier transform is also referred to as a Fourier spectrum, frequency spectrum or spectral density. The coordinates u and v in the Fourier transform domain are referred to as spatial frequency coordinates.

The Fourier transform has an inverse which is defined, for any complex function G of two independant variables u and v, by

$$F^{-1}\{G(u,v)\} = \int\int_{-\infty}^{\infty} G(u,v)\, \mathrm{Exp}[j2\pi(ux+vy)]\,dudv \qquad (2.2)$$

where $F^{-1}\{\ \}$ denotes "inverse Fourier transform of".

There exist several theorems expressing certain properties of Fourier transforms. Some of the most important of these theorems are:

1. Linearity Theorem.

If g and h are two complex functions of two independent variables x and y and a and b are complex constants then

$$F\{a\times g(x,y)+b\times h(x,y)\}=aF\{g(x,y)\}+bF\{h(x,y)\} \qquad (2.3)$$

2. Convolution Theorem.

If $F\{g(x,y)\}=G(u,v)$ and

$F\{h(x,y)\}=H(u,v)$ then

$$F\{\int\int_{-\infty}^{\infty} g(p,q)\,h(x-p,y-q)\,dpdq\}=G(u,v)\,H(u,v) \qquad (2.4)$$

The quantity inside the curly brackets on the left hand side of the equation is, by definition, the convolution of the functions g and h.

3. Fourier integral theorem.

If g(x,y) is a continuous function then

$$F\{F^{-1}\{g(x,y)\}\}=F^{-1}\{F\{g(x,y)\}\}=g(x,y) \qquad (2.5)$$

A statement of these theorems and others together with proofs is given in reference [13].

2.2 Linear Systems

In optical data processing one is frequently concerned with the relationship between a two-dimensional complex amplitude distribution (sometimes referred to simply as "light distribution") in the input plane of an optical system and that of the output plane of the system.

Any optical system can be represented as an operator P which acts on the input to produce the output.

Thus if $i(x_1,y_1)$ is the light distribution in the input plane and $o(x_2,y_2)$ is the light distribution in the output plane, the effect of the system can be expressed as

$$o(x_2,y_2)=P\{i(x_1,y_1)\} \tag{2.6}$$

As an example $i(x_1,y_1)$ could be the light distribution in the object plane of an imaging system and $o(x_2,y_2)$ the light distribution in the image plane.

A system is said to be linear if the following expression is true for all complex constants a and b and all inputs $i(x_1,y_1)$ and $j(x_1,y_1)$:

$$P\{a\times i(x_1,y_1)+b\times j(x_1,y_1)\} = aP\{i(x_1,y_1)\}+bP\{j(x_1,y_1)\} \tag{2.7}$$

The linearity of a system implies that any input can be decomposed into as many parts as desired provided only that the parts add up to the actual input.

The Dirac delta function is a convenient way of decomposing an input. The Dirac delta function may be defined by

$$\delta(x,y)=\lim_{N\to\infty} N^2\mathrm{Exp}[-N^2\pi(x^2+y^2)] \tag{2.8}$$

Making use of the Dirac delta function the input $i(x_1,y_1)$ to an optical system can be rewritten as

$$i(x_1,y_1)=\int\int_{-\infty}^{\infty} i(p,q)\,\delta(x_1-p,y_1-q)\,dpdq \qquad (2.9)$$

The property of the delta function which makes it so useful for the purpose of decomposition is called the sifting property and is discussed in detail in reference [13].

Combining equations (2.6) and (2.9) the output of a linear optical system can be written as

$$o(x_2,y_2)=\int\int_{-\infty}^{\infty} i(p,q)\,P\{\delta(x_1-p,y_1-q)\}\,dpdq \qquad (2.10)$$

In the above equation the linearity property has been used to bring the operator P under the integral. It should be pointed out that while the right hand side of equation (2.10) does not depend explicitly on x_2 and y_2, the result of the operation by P is a function of x_2 and y_2 as can be seen from equation (2.6).

The quantity $P\{\delta(x_1-p,y_1-q)\}$ is the output of the system due to an impulse (delta function) at coordinates (p,q) in the input plane. This is called the impulse response of the system and will be denoted by h. Thus

$$h(x_2,y_2,p,q)=P\{\delta(x_1-p,y_1-q)\} \qquad (2.11)$$

2.3 Space-Invariant Linear Systems

A system is said to be space-invariant if the impulse response does not depend explicitly upon all the coordinates x_2, y_2, p and q but only on the differences (x_2-p) and (y_2-q). In this case equation (2.10) becomes

$$o(x_2,y_2)=\int\int_{-\infty}^{\infty} i(p,q)\,h(x_2-p,y_2-q)\,dpdq \qquad (2.12)$$

Comparing equation (2.12) to equation (2.4), the right hand side of equation (2.12) is seen to be the convolution of i and h. From now on the convolution operation will be denoted by * and equation (2.12) can be rewritten as

$$o(x_2,y_2)=i*h \qquad (2.13)$$

Using the convolution theorem (2.4) equation (2.12) can be Fourier transformed:

$$O(u,v)=H(u,v)I(u,v) \qquad (2.14)$$

The upper case letters denote the Fourier transform of the functions indicated by the corresponding lower case letters.

Equation (2.12) is a space domain description of the system while (2.14) is a frequency domain description. H(u,v) is the Fourier transform of h(p,q), the system's impulse response, and is called the transfer function of the system.

2.4 Fourier Transformation by Lenses

Optical Filtering System

The computational task of calculating a Fourier transform is a rather complicated one for all but the simplest functions. However, a very simple optical system consisting only of a lens and free space can perform the two-dimensional Fourier transformation on any light distribution at a very high speed [14]. (Essentially the

time taken to perform the transformation is the time taken by light to travel from the input to the output of the optical system). This property of an optical lens makes it an extremely powerful tool for the purpose of optical spatial filtering.

Figure 1 shows an optical configuration which can be used for any spatial filtering task, including matched filtering.

Plane P1 contains $s(x_1,y_1)$, the input to the system, i.e. the pattern that is to be filtered. $s(x_1,y_1)$ is illuminated by a plane wave of amplitude a, so the complex light amplitude distribution $b(x_1,y_1)$ of the wave emerging from P1 is given by

$$b(x_1,y_1)=a\times s(x_1,y_1) \qquad (2.15)$$

The planes P1 and P2 are each separated from the plane of the (thin) lens by f, the focal length of the lens. Under these circumstances L1 performs a two-dimensional Fourier transformation on $b(x_1,y_1)$ [14] and the Fourier spectrum of $b(x_1,y_1)$ is displayed in plane P2. The light amplitude $c(x_2,y_2)$ at plane P2 is given by

$$c(x_2,y_2)=\frac{a}{j\lambda f}S(u,v) \qquad (2.16)$$

where $S(u,v)$ is the Fourier transform of $s(x_1,y_1)$ [14].

The spatial frequency coordinates (u,v) in plane

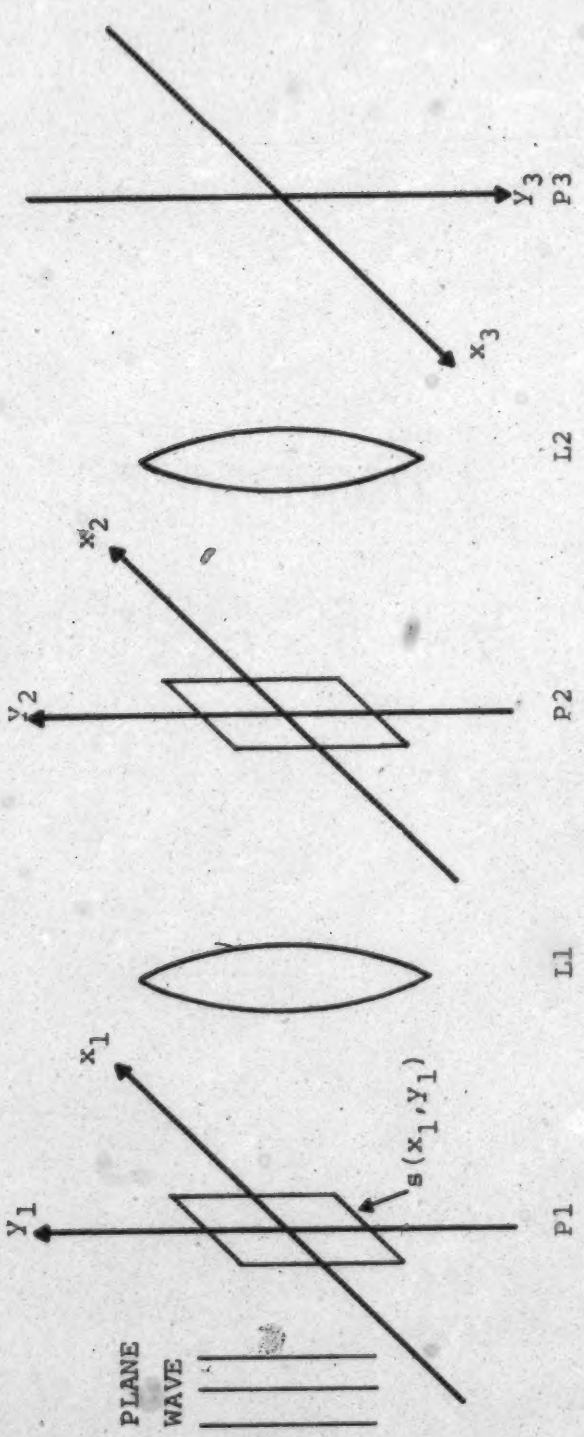

Figure 1. Optical filtering system.

P2 are related to the real coordinates (x_2,y_2) by

$$u=x_2/(\lambda f) \quad \text{and} \quad v=y_2/(\lambda f) \tag{2.17}$$

where λ is the wavelenght of the coherent plane wave which illuminates $s(x_1,y_1)$.

Whenever the light distribution in one plane of an optical system has a Fourier transform relationship with that of another plane of the system it is convenient to consider one of the planes in terms of the frequency coordinates. This is frequently done throughout the remainder of this thesis. Under these circumstances it must always be born in mind that the two types of coordinates are related by equation (2.17). The unit of the real coordinates is that of length whereas the unit of the spatial frequency coordinates is 1/(length). Coordinate-axis in figures in the thesis are labelled with the coordinates most frequently used in the text.

In spatial filtering the absolute amplitude of the Fourier transform in plane P2 is of little interest and thus the constant $a/(j\lambda f)$ in equation (2.16) is frequently dropped. Throughout the remainder of this thesis the constant will be neglected and thus $c(x_2,y_2)$ is assumed to be given by

$$c(x_2,y_2)=S(u,v) \tag{2.18}$$

A filter is introduced into plane P2 of Figure 1,

thereby altering the frequency content of $s(x_1,y_1)$. This modified spectrum is then Fourier transformed once more by lens L2 and the filtered version of $s(x_1,y_1)$ appears in plane P3.

The lens L2 performs a Fourier transformation whereas an inverse Fourier transform is required. Comparing equations (2.1) and (2.2) it is seen, however, that an inverse Fourier transform is in fact a Fourier transform in reflected coordinates. (x is replaced by -x and y by -y). This is the reason for the reflection of coordinates (x_3,y_3) in plane P3.

It should be pointed out that the transfer function of this optical system is simply the transmission function of the filter placed in plane P2.

2.5 The Matched Filter

A filtering system is said to be matched to a signal $s(x,y)$ if it has a transfer function given by $S'(u,v)$ [2]. $S(u,v)$ is the Fourier transform of the signal $s(x,y)$ and ' denotes a complex conjugate. Since the transfer function of the system shown in Figure 1 is the transmission function of the filter in plane P2, the above defintion implies that a filter matched to $s(x,y)$ must have transmission function $S'(u,v)$.

When a filter with transmission function $S'(u,v)$ is present in plane P2 and $s(x,y)$ is present at the input,

the light amplitude $d(x_2,y_2)$ behind plane P2 is given by

$$d(x_2,y_2)=S(u,v)S'(u,v) \tag{2.19}$$

The right hand side of equation (2.19) is necessarily a real quantity. This implies that the light amplitude distribution behind plane P2 has a constant phase throughout the plane i.e. is a plane wave. A plane wave emerging from plane P2 is focused to a point in plane P3.

If any transmission function other than $s(x,y)$ is present at the input, equation (2.19) is no longer true and the wave emerging from plane P2 is not a plane wave, and will not be focused to a point in plane P3. Since a spot of light in plane P3 indicates that $s(x,y)$ is present at the input or that $s(x,y)$ "has been recognized" at the input, it is referred to as a recognition spot. The above also explains why the filter is called a matched filter.

A matched filter can also be defined in terms of its impulse response. It is assumed that the filtering system is sapce-invariant and thus as can be seen from section 2.2 the impulse response of the system is given by the inverse Fourier transform of the transfer function.

It is a well known property of Fourier transforms [15] that

$$F\{s'(-x,-y)\}=S'(u,v) \tag{2.20}$$

where S(u,v) is the Fourier transform of s(x,y). A matched filter is then required to have an impulse response given by s'(-x,-y).

Consider now the optical system shown in Figure 2. Lens L1 Fourier transforms the spherical wave diverging from the point source in plane P1, so plane P2 is illuminated by a plane wave. Lens L2 performs an inverse Fourier transform on the light emerging from plane P2.

A matched filter can now be equivalently defined in terms of the optical system of Figure 2 as any mask which when introduced into plane P2 gives rise to s'(-x,-y) appearing in plane P3. Two comments should be made about the last definition of a matched filter. First, it is strictly required that s'(-x,-y) and <u>only</u> s'(-x,-y) appears in plane P2 when a filter matched to s(x,y) is present in plane P2. However, if s'(-x,-y) appears somewhere in P3 it is always possible to shield off any light distribution which may appear elsewhere in the plane. Secondly, since the system of Figure 2 is assumed to be space-invariant, the point source in plane P1 may be displaced off the optical axis. The only effect of this is to tilt the plane wave incident on P2 and to displace the complete light distribution in plane P3.

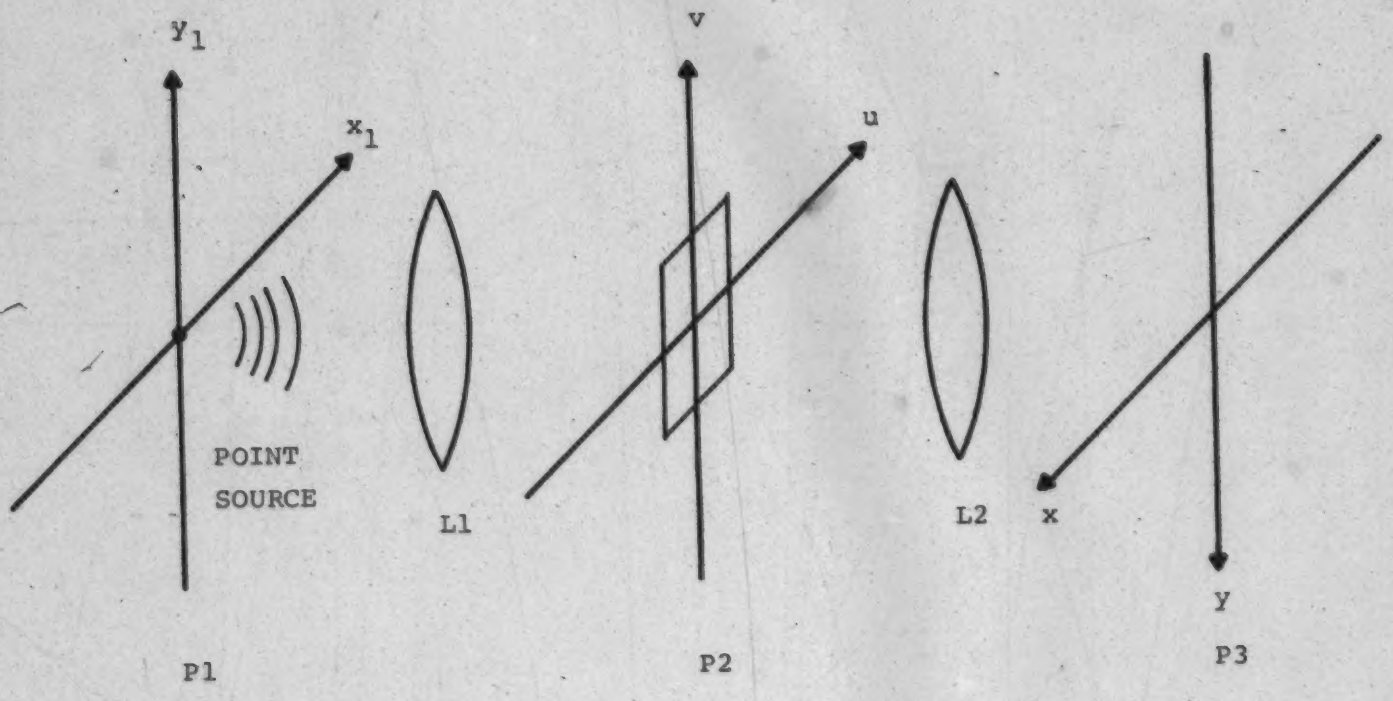

Figure 2. Optical system defining a matched filter.

2.6 Production of Matched Filters

In order to realize an optical matched filter it is required to produce a transparency with transmission function given by $S'(u,v)$. This is in general a complex function, i.e. it is required to control both the amplitude and phase of light passing through the filter.

While $S'(u,v)$ is a complex function, $S'+S$ is always a real function. Techniques exist by which $S'+S$ are recorded on photographic film in such a way that when the film is inserted into plane P2 of Figure 2, the responses in plane P3 due to the two terms S' and S are separated. Two of these techniques were outlined in Chapter 1, and will be examined in more detail in the next chapter.

CHAPTER 3

VANDER LUGHT AND LOHMAN FILTERS

3.1 The Vander Lught Filter

A Vander Lught filter is a photographic record of the interference fringes due to a light amplitude $S'(u,v)$ and a tilted plane wave.

Figure 3 shows a schematic diagram of an optical system which could be used to record a Vander Lught filter.

A more practical configuration is the modified Mach-Zehnder interferometer originally used by Vander Lught [3] and other configurations later shown by Vander Lught [16].

Referring to Figure 3, plane P1 contains a transparency with a transmission function $s'(-x,-y)$. This is the impulse response which the filter is required to have and is generally a real function. The lens performs a Fourier transformation on $s'(-x,-y)$ and displays $S'(u,v)$ in plane P2, the back focal plane of L.

The part of the plane wave which passes above the mask in P1 is deflected by means of the prism to strike the plane P2 at an angle θ. The complex amplitude resulting in plane P2 from this tilted plane wave (sometimes called a reference wave) is given by

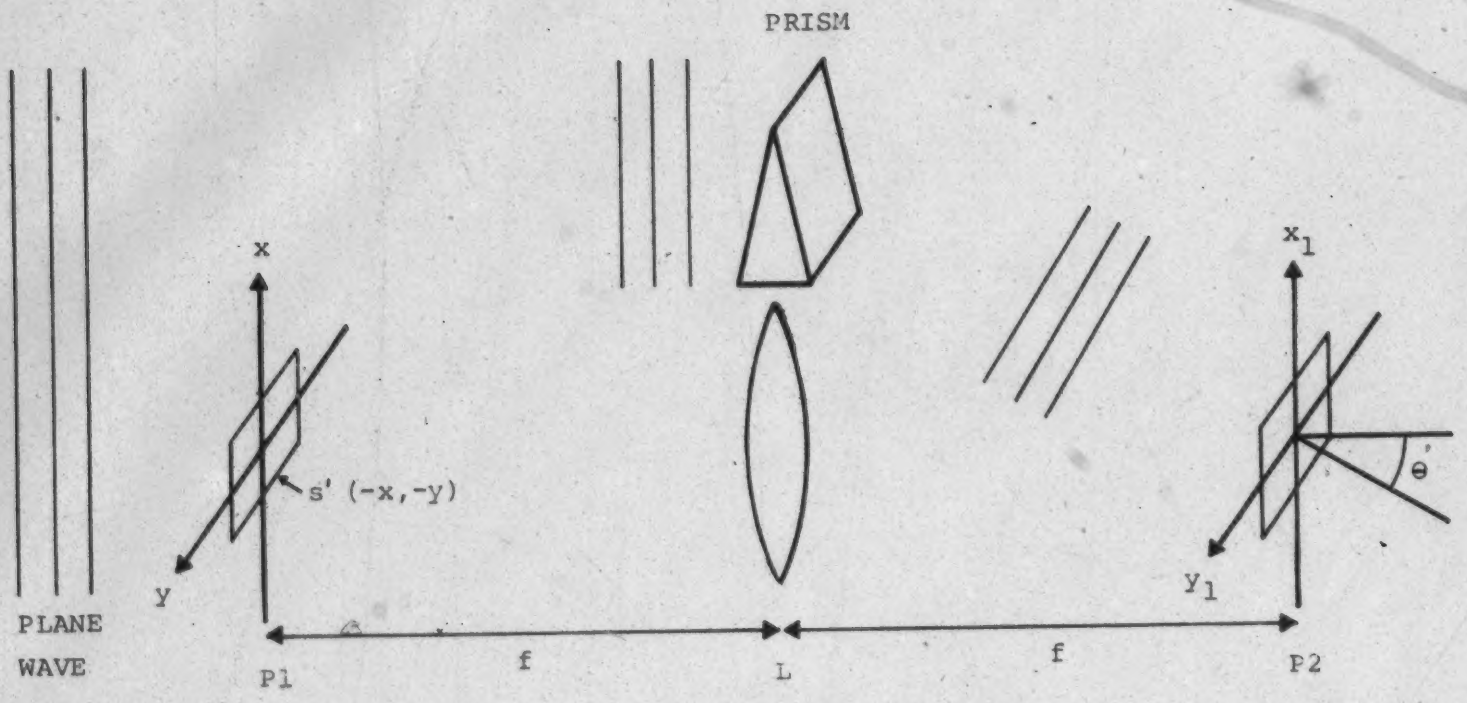

Figure 3. Optical system to record a Vander Lught filter.

$$r(x_1,y_1)=aExp(-j2\pi wx_1) \tag{3.1}$$

where a is the amplitude of the plane wave and w is given by [17]

$$w=(Sin\theta)/\lambda \tag{3.2}$$

and λ is the wavelenght cf light used.

To produce a Vander Lught filter, a photographic plate is inserted into plane P2 and exposed to the light amplitudes previously described.

It is assumed that after development, the plate will have transmittance proportional to the intensity of light which expcsed the plate. The transmission function of the finished filter can then be written as

$$T(u,v)=|aExp(-j2\pi wx_1)+S'(u,v)|^2 \tag{3.3}$$

In the above expression a constant of proportionality is neglected. Expanding equation (3.3) and replacing x_1 by $u\lambda f$ yields

$$T(u,v)=a^2+|S'(u,v)|^2+aS'(u,v)Exp(j2\pi w\lambda fu) + aS(u,v)Exp(-j2\pi w\lambda fu) \tag{3.4}$$

If the complex function S'(u,v) is separated into amplitude and phase by

$$S'(u,v)=A(u,v)Exp[-j\emptyset(u,v)] \tag{3.5}$$

the transmission function can be rewritten as

$$T(u,v)=a^2+A^2(u,v)+2aA(u,v)\cos[2\pi w\lambda f u-\phi(u,v)] \qquad (3.6)$$

Equations (3.4), (3.5) and (3.6) describe fully the transmission function of a Vander Lught filter.

Before these equations are considered more closely it will be shown that this filter does indeed satisfy the requirements for a matched filter in that the impulse response of the filter contains the term $s'(-x,-y)$ and this term can be separated from other terms in plane P3 of Figure 2.

Referring to Figure 2, when $T(u,v)$ is introduced into plane P2, the inverse Fourier transform of $T(u,v)$ appears in plane P3. Performing the inverse Fourier transformation on equation (3.4) (or equivalently Fourier transforming $T(u,v)$ and then replacing x by -x and y by -y) shows that $u(x,y)$, the light distribution in P3, is given by [17]

$$u(x,y)=a^2\delta(x,y)+s(x,y)*s'(x,y)$$
$$+as'(-x,-y)*\delta(x+w\lambda f,y)+as(x,y)*\delta(x-w\lambda f,y) \qquad (3.7)$$

Convolution of a function with a delta function results in the same function with an origin shifted to the location of the delta function [18]. Equation (3.7) therefore contains $s'(-x,-y)$ centered at $x=-w\lambda f$, $y=0$ and multiplied by the constant a. Furthermore, provided $s(x,y)$ is limited in

spatial extent this term can always, by an appropriate choice of w, be separated from the other terms of equation (3.7). The filter does therefore satisfy the requirements for a matched filter.

From equations (3.4) to (3.7) some of the properties of the Vander Lught filter can be deduced:

1) Comparing equations (3.4) and (3.7) it is seen that the first two terms in equation (3.4) do not contribute to the building up of $s'(-x,-y)$, the important part of the impulse response.

2) In order that $T(u,v)$ remains non-negative a, the amplitude of the reference wave, must be chosen at least as high as the highest amplitude of $S'(u,v)$.

3) The third term of equation (3.6) is both an amplitude and phase record of $S(u,v) + S'(u,v)$. Here it is seen how the two complex waveforms are recorded together as a real record.

4) If, during the recording of a filter, $s(x,y)$ is present in plane P1 of Figure 3 instead of $s'(-x,-y)$ it is found that equation (3.7) changes to

$$u(x,y)=a^2\delta(x,y)+s(x,y)*s'(x,y) + as(x,y)*\delta(x+w\lambda f,y)+as'(-x,-y)*\delta(x-w\lambda f,y) \quad (3.7a)$$

The light distribution in plane P2 is therefore the same as before, except the locations of $s(x,y)$ and $s'(-x,-y)$ have

been interchanged. This impulse response again satisfies the requirements for a matched filter and since s(x,y) is usually more readily available than s'(-x,-y), a Vander Lught filter is most often produced with s(x,y) in plane P1 of Figure 3 instead of s'(-x,-y).

3.2 The Lohman Filter

A.W. Lohman and co-workers have published several papers about their method of using a computer and a computer-guided plotter to produce holograms which amongst other uses can serve as matched filters.

The principle behind these holograms was first explained in terms of what the inventors have called the detour phase [8]. In a subsequent paper [9] a more detailed explanation of these filters was given and the function of the holograms examined in terms of diffraction theory.

The description of the Lohman filter that follows is mainly based on the two above mentioned publications.

The Lohman filter consists of a great number of rectangular apertures on an opaque background. The plane of the filter can be thought of as divided into a two-dimensional array of square cells with sides of length d. Each cell can be given two indices n and m to identify it. Let u and v be frequency coordinates in the plane of the filter and let the index n be increasing in the +u direction

and m be increasing in the +v direction.

Referring to Figure 4 each cell contains one aperture whose width in the u direction is given by cd. Its height in the v direction is $W_{nm}d$. The aperture is centered in the cell in the v direction but displaced by $P_{nm}d$ from the center of the cell in the u direction.

Since the filter is being described in terms of frequency coordinates, all distances in the plane of the filter have a unit of 1/(length).

The variables (filter parameters) W_{nm} and P_{nm} are to be selected in such a manner that the mask has the properties required of a matched filter.

The transmission function of such a mask can be written as [9]

$$T(u,v) = \sum_n \sum_m \text{Rect}\left[\frac{u-(n+P_{nm})d}{cd}\right] \text{Rect}\left[\frac{v-md}{W_{nm}d}\right] \qquad (3.8)$$

$\sum_n \sum_m$ indicates summation over all possible values of n and m and the Rect-function is defined by

$$\text{Rect}(x) = \begin{cases} 1 & \text{if } |x| \leq 1/2 \\ 0 & \text{if } |x| > 1/2 \end{cases} \qquad (3.9)$$

This filter is placed in plane P2 of the optical system shown in Figure 5 and illuminated by the tilted plane wave derived from a point source located at $x=x_o$ in plane P1.

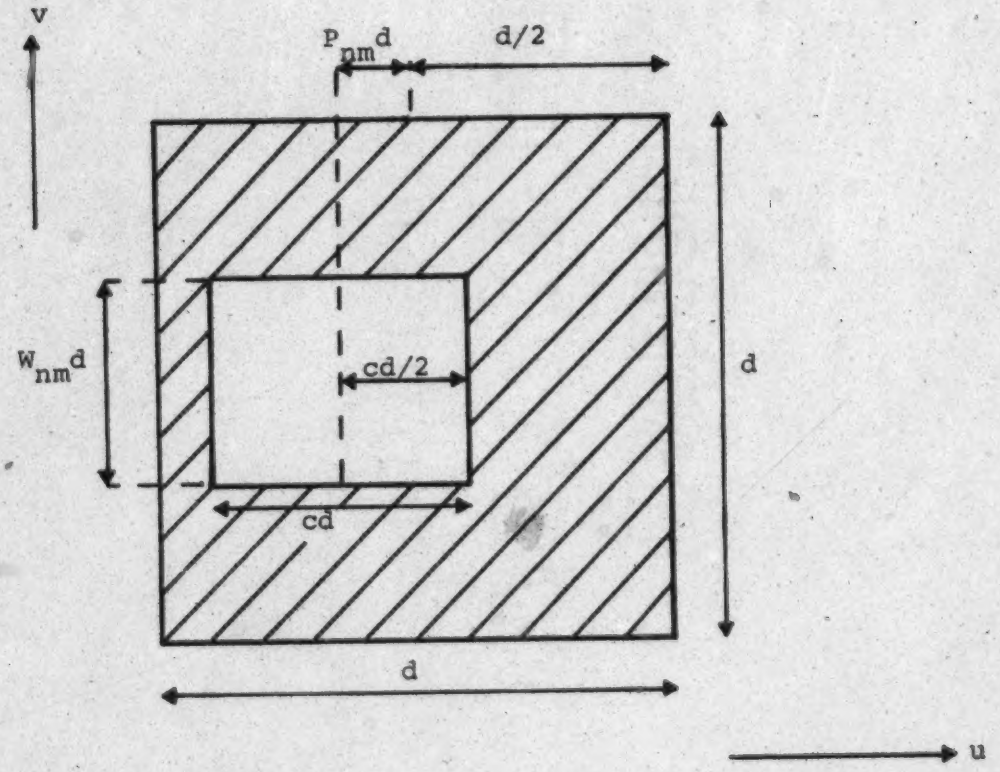

Figure 4. A cell of a Lohman filter.

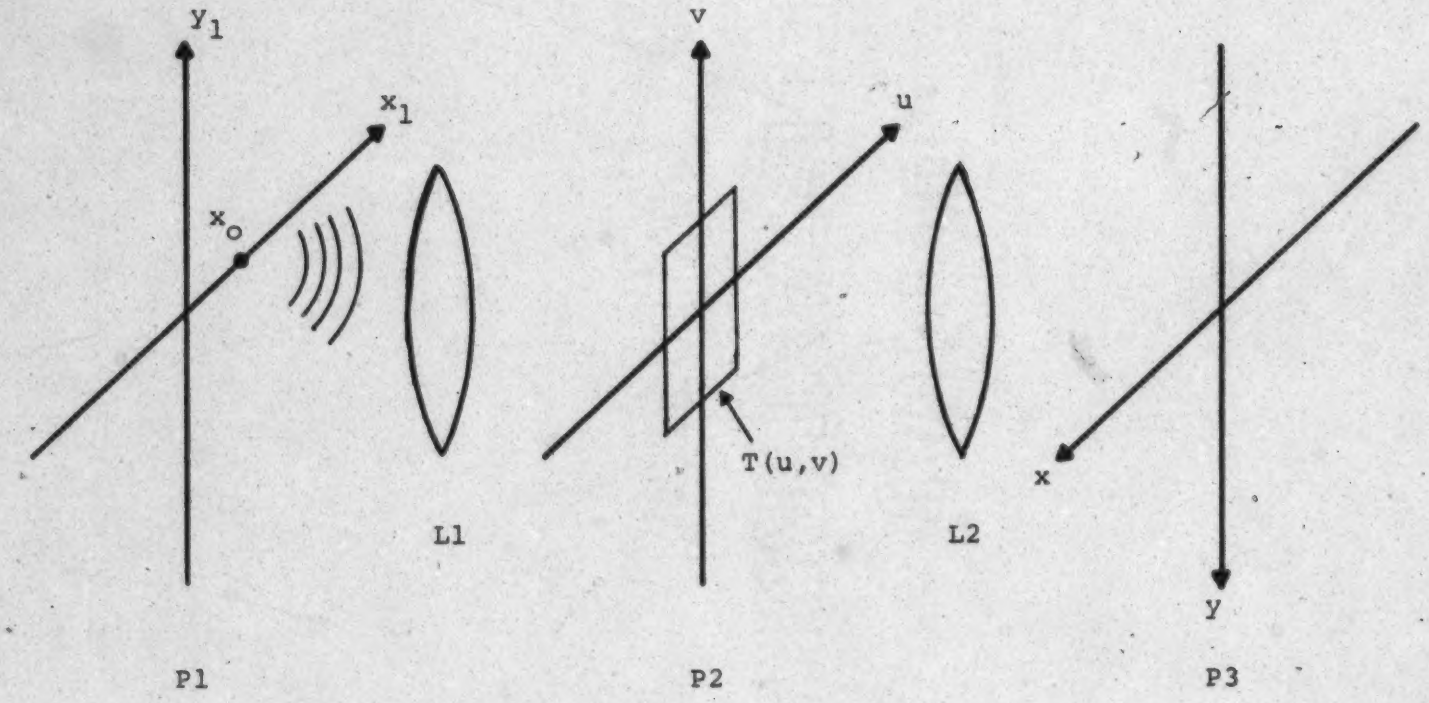

Figure 5. Matched filter illuminated by a tilted plane wave.

The problem at hand is to select the parameters P_{nm} and W_{nm} in such a way that $s'(-x,-y)$, the required impulse response, appears somewhere in plane P3.

The system shown in Figure 5 differs from that of Figure 2 only in that the point source in plane P1 is displaced off the optical axis in Figure 5 but is on the axis in Figure 2. As was pointed out in section 2.4 the displacement of the source off the axis results only in the complete light distribution in plane P3 being shifted. If therefore $s'(-x,-y)$ appears in plane P3 of Figure 5 it does also appear in plane P3 of Figure 2, only at a different location. Thus either system can be used to define a matched filter.

Assuming that the tilted plane wave has unit amplitude, the complex light amplitude of the wave emerging from P2 is equal to [9]

$$B(u,v)=T(u,v)\,\mathrm{Exp}(j2\pi x_o u) \tag{3.10}$$

The inverse Fourier transform of this amplitude appears in plane P3. This is given by

$$b(x,y)=F^{-1}\left\{\sum_n\sum_m \mathrm{Rect}\left[\frac{u-(n+P_{nm})\,d}{cd}\right]\mathrm{Rect}\left[\frac{v-md}{W_{nm}d}\right]\mathrm{Exp}(j2\pi x_o u)\right\} \tag{3.11}$$

The above transformation is carried out in Appendix A and it is shown that $b(x,y)$ is given by

$$b(x,y) = cd^2 \mathrm{Sinc}[(x+x_o)cd] \times$$
$$\sum_n \sum_m W_{nm} \mathrm{Sinc}(yW_{nm}d) \mathrm{Exp}\{-j2\pi d[(n+P_{nm})(x+x_o)+my]\} \quad (3.12)$$

where the Sinc function is defined by

$$\mathrm{Sinc}(x) = \frac{\mathrm{Sin}(\pi x)}{\pi x} \quad (3.13)$$

To establish that the Lohman mask is suitable for use as a matched filter, it must be shown that $b(x,y)$ in equation (3.12), is at least approximately equal to $s'(-x,-y)$ somewhere in plane P3 of Figure 5.

Let it be assumed that $s'(-x,-y)$ is limited in spatial extent such that it is completely contained within a rectangular window $w(x,y)$. The window $w(x,y)$ has sides of length L_x and L_y in the x and y directions respectively and is given by

$$w(x,y) = \mathrm{Rect}(x/L_x)\,\mathrm{Rect}(y/L_y) \quad (3.14)$$

Then it is required to show that

$$w(x,y)\,b(x,y) \approx s'(-x,-y) \quad (3.15)$$

The symbol $\approx$ means "approximately equal to".

In order to establish relationship (3.15) some approximations must be made to $b(x,y)$ in equation (3.12). The approximations made by Lohman are the following:

$$\begin{aligned} &1)\quad \mathrm{Sinc}\{(x+x_o)cd\}\simeq 1 \quad \text{for } |x|\le L_x/2 \\ &2)\quad \mathrm{Sinc}\{(yW_{nm}d\}\simeq 1 \quad \text{for } |y|\le L_y/2, \text{ all } W_{nm} \\ &3)\quad \mathrm{Exp}(j2\pi xP_{nm}d)\simeq 1 \quad \text{for } |x|\le L_x/2, \text{ all } P_{nm} \end{aligned} \tag{3.16}$$

Lohman has given both theoretical and experimental justifications for these approximations which are discussed in detail in reference [9]. Adopting these approximations, equation (3.12) becomes

$$b(x,y)=cd^2\sum_n\sum_m W_{nm}\mathrm{Exp}\{-j2\pi d[(n+P_{nm})x_o+nx+my]\} \tag{3.17}$$

The above expression is seen to express $b(x,y)$ in terms of a Fourier series, so in order to facilitate comparison of $b(x,y)$ and $s'(-x,-y)$ the latter will first be expressed as a Fourier integral

$$s'(-x,-y)=\int\!\!\int_{-\infty}^{\infty}S'(u,v)\mathrm{Exp}\{-j2\pi(xu+yv)\}\,dudv \tag{3.18}$$

and finally $s'(-x,-y)$ is approximated by a sampled version of the above infinite series

$$s'(-x,-y)\simeq d^2\sum_n\sum_m S'(nd,md)\mathrm{Exp}\{-j2\pi d(xn+ym)\} \tag{3.19}$$

The right hand sides of equations (3.17) and (3.19) can now be equated term by term which results in

$$d^2S'(nd,md)=cd^2W_{nm}\mathrm{Exp}[-j2\pi d(n+P_{nm})x_o] \tag{3.20}$$

or if S' is written in amplitude and phase form

$$S'(nd,md)=A_{nm}\text{Exp}\{-j\phi_{nm}\} \tag{3.21}$$

where A_{nm} and ϕ_{nm} are the amplitude and phase respectively of $S'(u,v)$ at a point (nd,md) in the u,v plane. Now equation (3.19) can be rewritten as

$$W_{nm}=A_{nm}/c \tag{3.22}$$

and

$$\text{Exp}\{-j\phi_{nm}\}=\text{Exp}\{-j2\pi d(n+P_{nm})x_o\} \tag{3.23}$$

This last equation can be simplified if x_o is chosen such that $x_o d$ is an integer, K. Equation (3.22) can then be written as

$$\begin{aligned} W_{nm} &\propto A_{nm} \\ P_{nm} &= \phi_{nm}/(2\pi K) \end{aligned} \tag{3.24}$$

These last two equations determine the values of P_{nm} and W_{nm} such that the Lohman mask does act as a matched filter. It still remains to select values for the free constants K and c. The physical importance of these constants will be much more easily understood when the relationship of Lohman and Vander Lught filters has been established. At this point it will only be noted that the values Lohman most frequently uses for these constants are K=1 and c=1/2.

In summary, a Lohman filter is realized in the following way:

1) The Fourier transform of the required impulse response is computed in a digital computer, usually

according to the fast Fourier transform algorithm due to Cooley and Tukey [19]. The value of the Fourier transform is computed for n x m points spaced on a regular grid.

2) An array of n x m apertures is drawn on paper. The size and shapes of the apertures are described previously, in particular by Figure 4 and relationship (3.24).

3) The plot is photoreduced to the required size.

3.3 The Relationship between Vander Lught and Lohman Filters

It has been suggested [20] that the Lohman filter is the spatial equivalent of pulse modulation while the Vander Lught filter is based on amplitude and phase modulation of a sinusoidal carrier. However, nowhere in the literature is it shown what the relationship between a Vander Lught and a Lohman filter is.

In this section the transmission properties of the two filters will be analyzed and compared. The analysis will be conducted in the following way. The light amplitudes which expose a photographic plate during the recording of a Vander Lught filter are analyzed and $S'(u,v)$, the part of the light amplitude which is derived from $s'(-x,-y)$, is approximated by a piecewise continuous function (equation (3.28)). This allows the Vander Lught filter to be approximated by an array of cells, each having a sinusoidally varying transmission function (equation (3.37)). Finally these sinusoidal transmission functions

of the cells in the Vander Lught filter are approximated by binary transmission functions and they compared with the transmission functions of cells in a Lohman mask. The conclusion of the analysis is that the Lohman filter can be regarded as a binary approximation to the Vander Lught filter.

In section 3.1 it was seen that the Vander Lught filter is the photographic recording of a complex amplitude given by

$$C(u,v)=a\mathrm{Exp}(-j2\pi w\lambda f u)+S'(u,v) \tag{3.25}$$

The variables are the same as defined in section 3.1 and $S'(u,v)$ could alternatively be written as (see equation (3.5))

$$S'(u,v)=A(u,v)\mathrm{Exp}\{-j\phi(u,v)\} \tag{3.26}$$

Throughout the following analysis it must be born in mind that the spatial frequency coordinates (u,v) in the plane of the filter are related to the real coordinates (x,y) in that plane by $u=x/\lambda f$ and $v=y/\lambda f$. Thus the unit of the real coordinates (x,y) is that of length, whereas the unit of the frequency coordinates (u,v) is 1/(length).

Let it be assumed that $s'(-x,-y)$ is frequency-bandlimited so that $S'(u,v)$ is zero outside some rectangle in the u,v plane and consequently the filter has finite dimensions. Thus it is assumed that the Vander Lught

filter is contained within a rectangular window E(u,v) in the u,v plane. This window is further divided into n x m cells, each having sides of length d in the spatial frequency domain. Thus the window E(u,v) can be expressed as

$$E(u,v) = \sum_n \sum_m \text{Rect}\left[\frac{u-nd}{d}\right] \text{Rect}\left[\frac{v-md}{d}\right] \tag{3.27}$$

Further, it is assumed that d is so small that S'(u,v) is almost constant within each cell, and the continuous function S'(u,v) is replaced in each cell by its value in the middle of the cell

$$S'(u,v) \simeq \sum_n \sum_m S'(nd,md)\, \text{Rect}\left[\frac{u-nd}{d}\right] \text{Rect}\left[\frac{v-md}{d}\right] \tag{3.28}$$

With the above approximations the complex amplitude of the wave incident on the photographic plate in plane P2 of Figure 3 when the Vander Lught filter is being recorded, is written as

$$C(u,v) = a\text{Exp}\{-j2\pi w\lambda f u\} + \sum_n \sum_m S'(nd,md)\, \text{Rect}\left[\frac{u-nd}{d}\right] \text{Rect}\left[\frac{v-md}{d}\right] \tag{3.29}$$

In equation (3.29) w is related to θ, the tilting angle of the reference wave indicated in Figure 3, by equation (3.2). In order that the reference wave has the same distribution across each cell in the Vander Lught filter, let θ be chosen in such a way that

$$w\lambda fd=K \tag{3.30}$$

where K is an integer.

By inspection of equation (3.29), it is readily seen that this choice of θ means that the periodic reference wave distribution has an integral number of periods inside each cell of width d. Furthermore, the absolute phase of the reference wave depends on the time-origin, which can be chosen at will. Let the time-origin be chosen in such a way that the phase of the reference wave is π at the left hand side of any one cell. Since there is an integral number of periods inside each cell, this choice of time-origin ensures that the phase at the left hand side of each cell is π. Finally, a new coordinate x_n is introduced for each cell. This new coordinate has an axis parallel to the u axis and $x_n=0$ at the left hand side of each cell. Thus x_n is a coordinate common to all cells with the same value of the index n but a different value for m.

In terms of the x_n coordinates the distribution of the reference wave can be written as

$$a\mathrm{Exp}\{-j2\pi w\lambda fu\}= \sum_n \mathrm{Rect}\left[\frac{u-nd}{d}\right] a\mathrm{Exp}\{-j2\pi Kx_o/d-j\pi\} \tag{3.31}$$

Figure 6 shows the real part of equation (3.31) plotted as a function of the coordinate x_n. The plot extends over several cells in the u direction, and the value of K has been taken as 2.

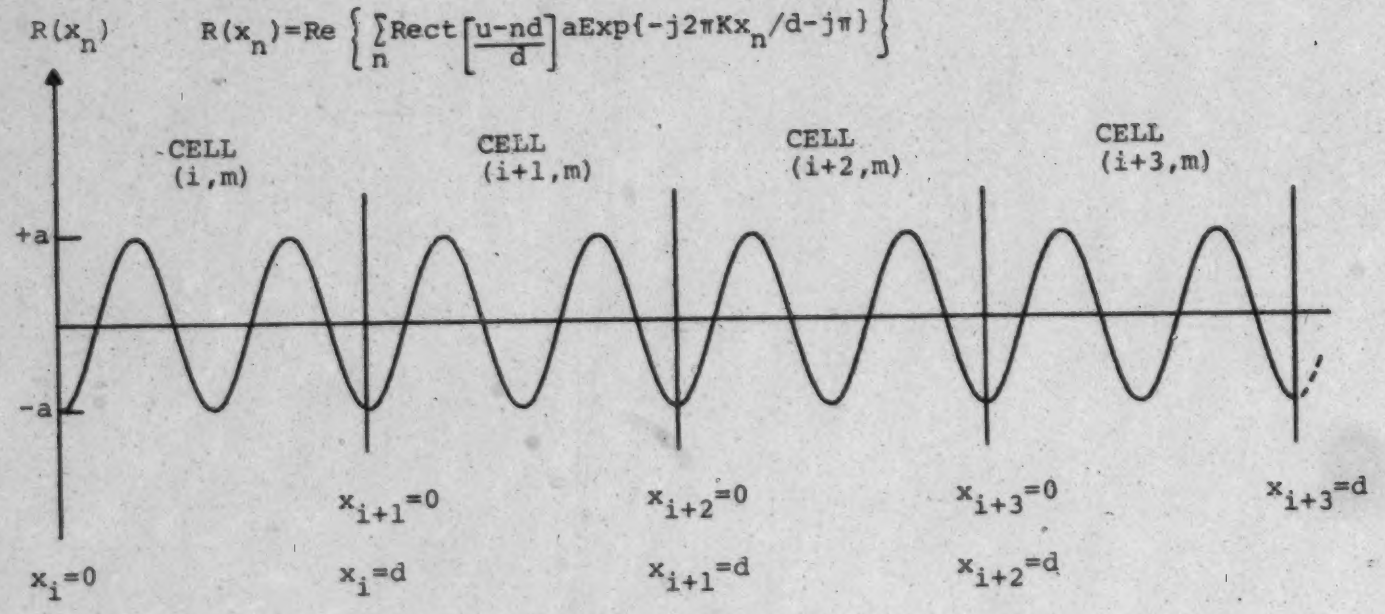

Figure 6. Plot of the real part of the reference wave distribution as a function of x_n.

Expressing the reference wave as in the right hand side of (3.31) allows it to be brought under the summation sign in equation (3.29) which results in

$$C(u,v)=\sum_n \sum_m \text{Rect}\left[\frac{u-nd}{d}\right]\text{Rect}\left[\frac{v-md}{d}\right]C_{nm}(u,v) \tag{3.32}$$

where

$$C_{nm}(u,v)=S'(nd,md)+a\text{Exp}\{-j2\pi Kx_n/d-j\pi\} \tag{3.33}$$

After development of the photographic plate the transmission function of the Vander Lught filter is given by

$$\begin{aligned} T(u,v)&=|C(u,v)|^2 \\ &=\left|\sum_n \sum_m \text{Rect}\left[\frac{u-nd}{d}\right]\text{Rect}\left[\frac{v-md}{d}\right]C_{nm}(u,v)\right|^2 \end{aligned} \tag{3.34}$$

At any given point in the u,v plane, only one set of Rect-funtions has a non-zero value. Consequently, in squaring the sum of equation (3.34) no cross terms appear. Furthermore, since a Rect-function only has the values zero and one, the square of a Rect-function is equal to the function itself. Thus expanding equation (3.34), T(u,v) becomes

$$T(u,v)=\sum_n \sum_m \text{Rect}\left[\frac{u-nd}{d}\right]\text{Rect}\left[\frac{v-md}{d}\right]\left|C_{nm}(u,v)\right|^2 \tag{3.35}$$

Squaring the modulus of equation (3.33) yields

$$\begin{aligned} \left|C_{nm}(u,v)\right|^2=a^2&+aS'(nd,md)\,\text{Exp}\{j2\pi Kx_n/d+j\pi\} \\ &+aS(nd,md)\,\text{Exp}\{-j2\pi Kx_n/d-j\pi\} \end{aligned} \tag{3.36}$$

If S' is written in terms of amplitude and phase as in equation (3.21), T(u,v) can be written as

$$T(u,v)= \sum_n \sum_m \text{Rect}\left[\frac{u-nd}{d}\right] \text{Rect}\left[\frac{v-md}{d}\right] \left[a^2+A_{nm}^2 +2aA_{nm}\text{Cos}\{2\pi(Kx_n/d+1/2)-\phi_{nm}\}\right] \quad (3.37)$$

The transmission function expressed in equation (3.37) is seen to vary in one direction only within each cell. This is the x_n (or u) direction. A cross-section of the transmission function indicated by equation (3.37) is plotted in Figure 7 as a function of x_n. In Figure 7, K has been given the value 1 and ϕ_{nm} is taken as $\pi/4$.

It was explained earlier that K determines the number of periods of the cosine-funtion within each cell and by inspection of (3.37) it is seen that ϕ_{nm} determines the phase of the cosine-function. Referring to Figure 7, the distance $G_{nm}d$ by which the maximum of the cosine function deviates from the middle of the cell, and H_{nm}, the peak to peak amplitude of the sinusoidal transmission function, are given by

$$G_{nm}=\phi_{nm}/(2\pi K) \quad \text{and} \quad H_{nm}=4aA_{nm} \quad (3.38)$$

In secion 3.1 (c.f. equations (3.4) and (3.7)) it was seen that the constant term D given by

$$D=a^2+A_{nm}^2 \quad (3.39)$$

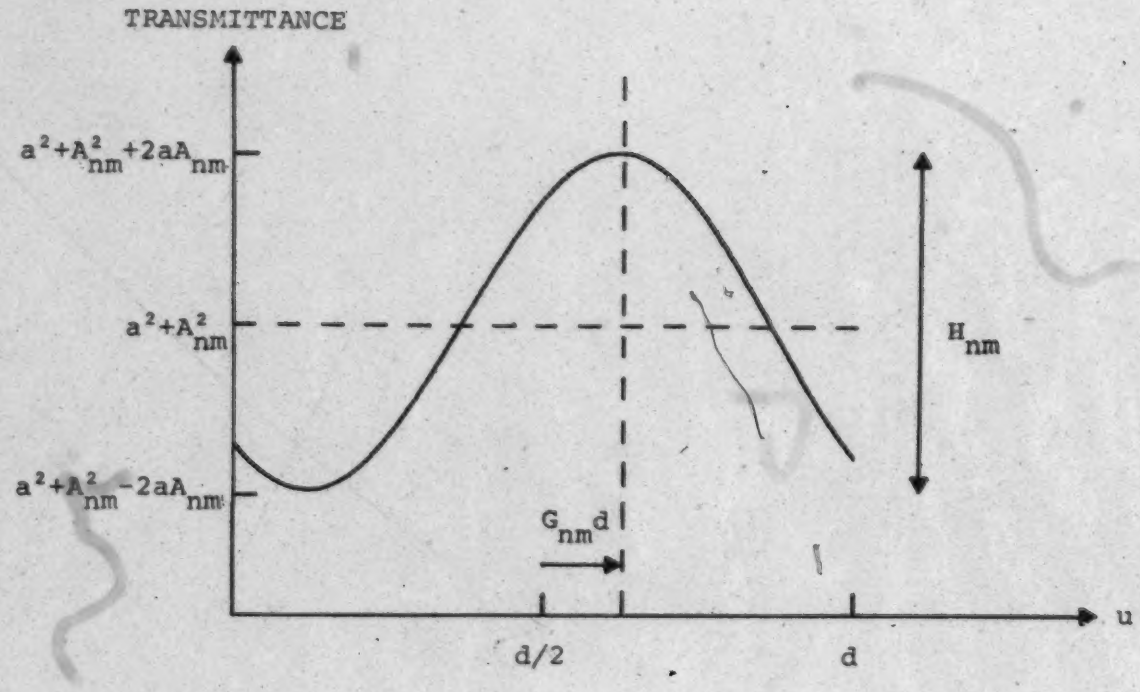

Figure 7. The transmission function of a cell in the approximation to a Vander Lught filter.

did not contribute to the part of the impulse response which was necessary for a matched filter. The importance of the constant D was to prevent the transmission function from becoming negative. If therefore the transmission function of each cell is reduced by a constant amount, such that it still remains positive or zero, the properties with respect to a matched filter have not changed. For this reason the modified transmission function shown in Figure 8 is equally valid as the one in Figure 7.

Finally, in order to produce a binary filter it is required to approximate the continuous tone transmission function by a binary transmission function, i.e. an opaque mask with some transparent areas.

There are many ways in which the sinusoidal transmission function of each cell can be approximated by one aperture in each cell. One of these is to use the arrangement previously described for a Lohman filter, and is drawn in Figure 4.

If the arrangement of Figure 4 is used to approximate the transmission function of Figure 8, the following requirements should be met:

1) The total amplitude of light coming from the aperture must be proportional to H_{nm}.

2) The aperture should be centered in the same location as the peak of the cosine wave, that is a distance $G_{nm}d$ from the middle of the cell.

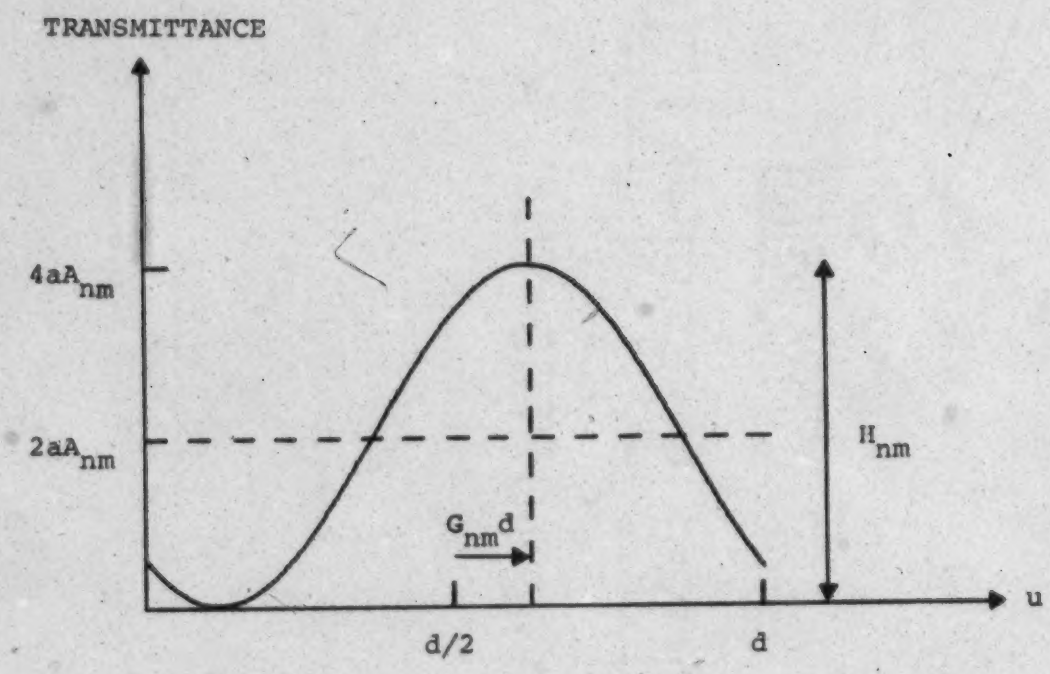

Figure 8. Modified transmission function of a cell in the approximation to a Vander Lught filter.

Since W_{nm} determines the total amplitude coming from the aperture in Figure 4 and P_{nm} determines the displacement of the aperture from the middle of the cell in the u direction, these two requirements imply the following relationship between W_{nm} and H_{nm}, and between P_{nm} and G_{nm}

$$W_{nm} \propto H_{nm}$$
$$P_{nm} = G_{nm} \qquad (3.40)$$

Since $H_{nm} \propto A_{nm}$ and G_{nm} is equal to $\phi_{nm}/(2\pi K)$ it is seen that equation (3.40) expresses the same choice of filter parameters P_{nm} and W_{nm} as Lohman arrived at by diffraction theory (equation (3.24)).

In conclusion, the analysis of a Vander Lught filter has resulted in a binary version of the filter which has the same filter parameters as Lohman derived by a completely different approach. Thus it has been established that the Lohman mask may be regarded as a binary approximation to a Vander Lught filter.

3.4 Discussion

Now that the relationship between Lohman and Vander Lught filters has been established the free constants, K and c, of the Lohman filter can be examined in terms of a Vander Lught filter.

As was indicated in section 3.3 the choice of K as an integer was to make sure that the reference wave has an

integral number of periods within each cell. This requirement leads to a simplification in the computation of the filter since the reference wave distribution is the same for each cell. K=1 implies that there is only one aperture in each cell which is obviously more convenient to plot than for example two apertures as in the case when K=2. However, as seen from equations (3.2) and (3.30) K is related to the tilting angle of the reference wave and thus also to the separation of $s'(-x,-y)$, the required part of the impulse response, from the spurious parts (c.f. equation (3.7)). Thus K=1 is an appropriate choice only if the separation so obtained is sufficient.

The choice of c=1/2 means that the cosine wave in Figure 8 is approximated by a square wave. This choice is intuitively easily understood. Other choices are, however, possible and have in some cases been made by Lohman [8].

A choice of K=1 and c=1/2 leads to a problem which by Lohman is referred to as the overlap problem. To explain this, consider a cell with $P_{nm}=1/2$. It is seen by considering Figure 4 that the aperture of this cell would extend into the adjacent cell by d/4. If now the adjacent cell happened to have $P_{n+1\ m}=-1/2$, then the two apertures would completely overlap. This problem is easily understood in terms of the present analysis of the Vander Lught filter and can be corrected. Figure 9 shows the transmission function of a cell in a Vander Lught filter

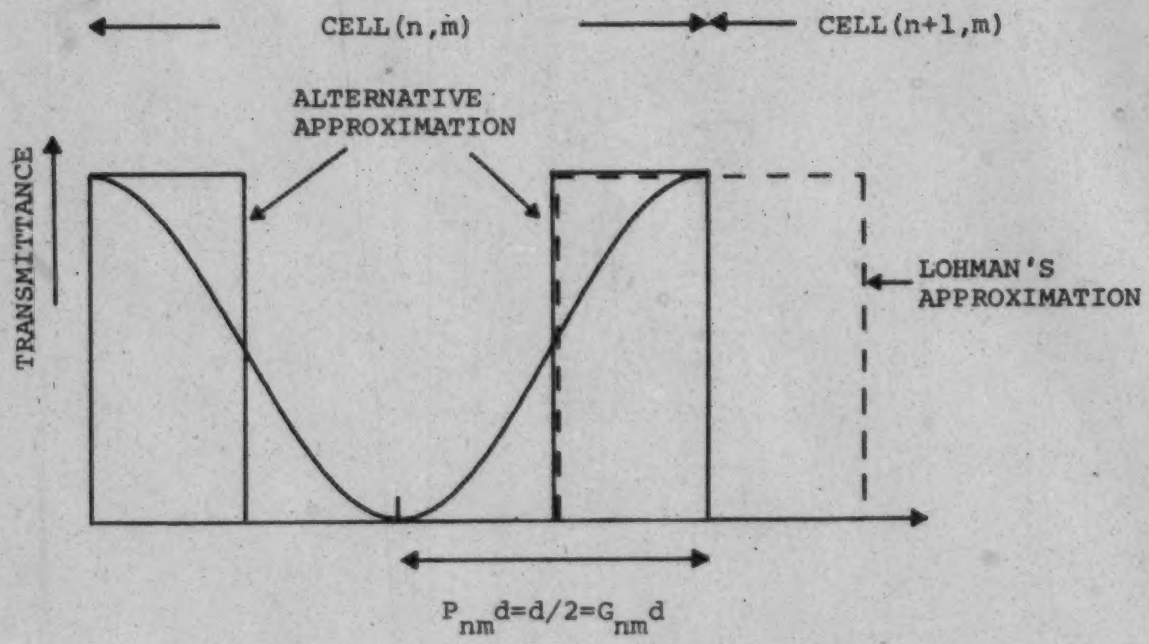

Figure 9. Approximations to the transmission function of a cell in a Vander Lught filter. $P_{nm}=G_{nm}=1/2$.

which would lead to $P_{nm}=1/2$, and it also shows how a Lohman filter approximates the transmission function. It is seen that the aperture extends into the adjacent cell. The problem of overlapping can be eliminated by choosing the alternative approximation to the Vander Lught transmission function drawn in Figure 9. Using this alternative approximation the aperture is divided into two parts, and is completely contained within one cell.

It has now been established that the Lohman and Vander Lught filters are equivalent, in that one can be regarded as a binary approximation of the other. The choice as to which filter is to be used in a matched filtering experiment does therefore depend primarily on the particular application and which of the two filters is more easily produced.

CHAPTER 4

SAMPLING CONSIDERATIONS

4.1 Introduction

Despite the equivalence of a Lohman and a Vander Lught filter which has been explained in the previous chapter, there is an important difference in their production. While the Vander Lught filter is made using optical methods only, the production of a Lohman filter requires that the signal to be matched, $s(x,y)$, is sampled at regular intervals and the resulting array of numbers Fourier transformed using a digital computer.

Prior to an algorithm due to Cooley and Tukey [19], known as the fast Fourier transform (FFT) algorithm, the Fourier transforming of large arrays of numbers was a very time consuming computation, so that the evaluation of Lohman masks would have been highly unpractical.

The FFT algorithm is a very efficient way of computing the Fourier transform of sampled data. A program written according to this algorithm requires as an input 2^n (n being an integer) equally spaced samples of a signal whose Fourier transform is required. The program then Fourier transforms the array of samples, returning 2^n frequency components equally spaced in the frequency space. The highest (+ve and -ve) frequency obtained is $1/(2X)$ where X is the distance between samples, or in the case of time

series, Δ is the time interval between samples.

Even when a fast Fourier transform algorithm is used, computing and plotting costs increase rapidly as the number of datapoints increases. The number of arithmetic operations required to compute the Fourier transform using conventional techniques is proportional to N^2 whereas using FFT they are proportional to $2N\log_2 N$ [21]. N is the number of samples to be transformed.

Using the IBM 360/67 computer belonging to the Department of Computing Services, University of Alberta, it takes approximately 15 seconds (CPU-time) to compute the Fourier transform of a 128x128 array using the FFT algorithm. It would take approximately two hours to compute this transform using conventional techniques. For a 256x256 array the figures would be 1 minute and 36 hours respectively.

Using the Calcomp 663 plotter belonging to Computing Services the plotting time for a 128x128 cell Lohman filter is approximately 1 hour, and for a filter of 256x256 cells the plotting time would thus be about 4 hours.

To give an indication of the cost of making a Lohman filter, the current rates for the computing facilities at this University are as follows: computing time (central processing unit) $600/hour, Calcomp plotter $16/hour. As a rough estimate, central processing unit

storage costs during execution are similar to the cost of computing time used.

The rates quoted above are the ones commercial non-university establishments are charged. At these rates the cost of computing and plotting a 128x128 cell Lohman filter can be estimated as $20 and the cost of a 256x256 cell filter would be about $85. The number of samples necessary to give a good representation of a signal is therefore an important factor in the production of a Lohman filter.

In this chapter the sampling requirements for a Lohman filter will be examined, using fingerprints as test patterns.

The reason for using fingerprints as test patterns is, as mentioned in Chapter 1, that the work done on fingerprint identification using Vander Lught filters [5,6] indicates that fingerprints are well suited for detection by matched filters and unlike manmade objects, such as alphanumeric characters, fingerprints seem to possess the arbitrariness common to many naturally occurring objects.

4.2 Sampling Theorem - Aliasing

It is required to use the fast Fourier transform algorithm to compute the Fourier transform of s(x,y). To this end s(x,y) is sampled over a regular grid of sampling points, spaced a distance X apart in the x direction and a

distance Y apart in the y direction. The array of samples a(x,y) so obtained can be written as

$$a(x,y) = \sum_n \sum_m s(x,y)\,\delta(x-nX, y-mY) \qquad (4.1)$$

The FFT algorithm can be used to compute the Fourier transform of a(x,y) which is also known as the discrete (or finite) Fourier transform of s(x,y). The question arises, how accurately the discrete Fourier transform approximates the continuous Fourier transform of s(x,y). The answer to this question is given by sampling theory:

If s(x,y) is a continuous function and a(x,y) is related to s(x,y) by equation (4.1), then the frequency spectra A(u,v) and S(u,v) of the two functions are related by [18]

$$A(u,v) = [1/(XY)] \sum_n \sum_m S(u-n/X, v-m/Y) \qquad (4.2)$$

The right hand side of equation (4.2) is proportional to an array of functions equal to S(u,v) centered at (n/X, m/Y) where n and m can have any values between $-\infty$ and ∞. Thus the nearest S(u,v) functions are separated by 1/X and 1/Y in the u and v directions respectively.

If s(x,y) is a bandlimited function then S(u,v) is non-zero only in a limited region of the frequency plane. Let it be assumed that s(u,v) is non-zero only for frequencies $|u|<W$ and $|v|<W$. Under these conditions the

various S(u,v) functions in equation (4.2) are separated provided X and Y are chosen such that

$$X<2W \quad \text{and} \quad Y<2W \tag{4.3}$$

The situation described above is drawn in Figure 10a for the part of the spectrum along the line v=0. Only the central part of the infinite array of S(u,v) functions is shown.

Suppose now that X is increased such that the relationship (4.3) is no longer true. Then as is shown in Figure 10b the various S(u,v) terms are no longer separated but overlap. Thus it is no longer possible to recover S(u,v) exactly from A(u,v). The damage to S(u,v) is referred to as aliasing and it is said that high frequency components from an adjacent S(u,v) function alias high frequency components of the central S(u,v) function.

Prior to the experiments with fingerprint identification described here, some experiments were done with Lohman filters in character recognition. In these experiments the problem of aliasing was quite apparent.

Figure 11 shows the amplitude of the Fourier transform of the letter A, computed using the FFT algorithm. The computed Fourier transform is composed of 128x128 datapoints. Each of the datapoints is represented in Figure 11 by a black square, the area of the square being proportional to the amplitude of the Fourier transform at

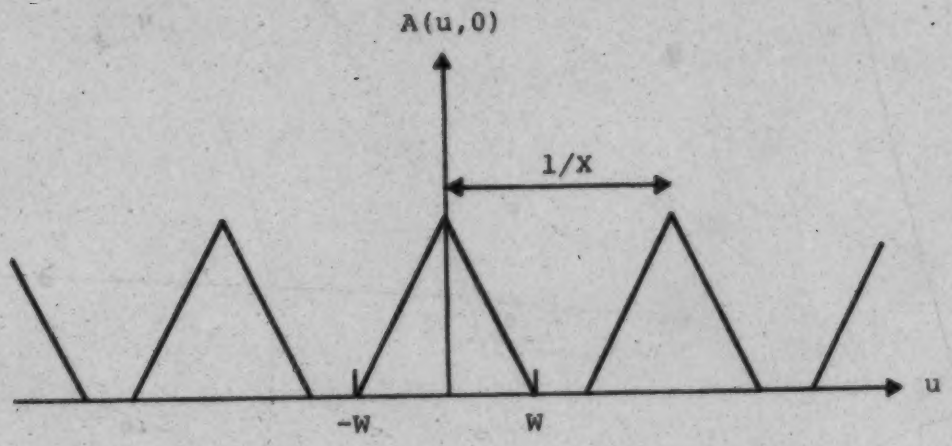

(a) No aliasing present.

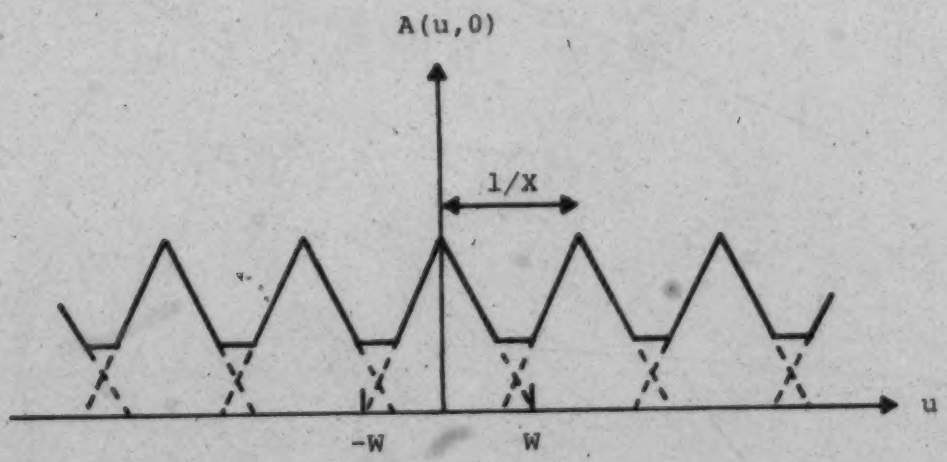

(b) Aliasing present.

Figure 10. The spectrum of a sampled signal.

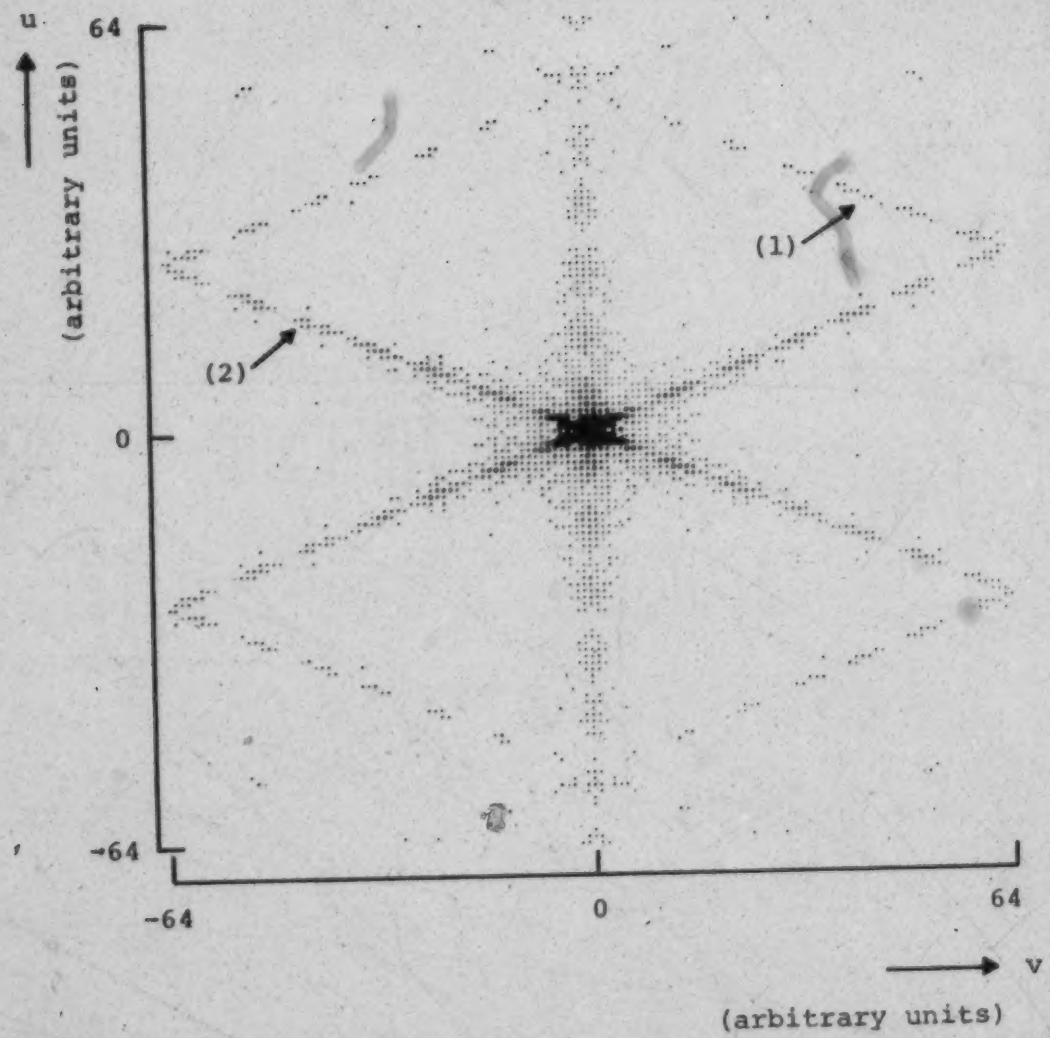

Figure 11. Computed Fourier transform of the letter A.

that point.

When the computed Fourier transform of Figure 11 was compared with the optically obtained Fourier transform of the same letter A, it was found that the line of spectral components indicated by (1) in Figure 11 was in fact the continuation of the line (2) from an adjacent spectrum, appearing in the central spectrum because of aliasing.

Intuitively one might suspect that fingerprints, being complicated patterns, possessed a wide range of spatial frequencies. If this was the case, it would be necessary to employ a great number of samples to adequately discribe a given area of a fingerprint. This would lead to high computing costs and thus render the Lohman filter very uneconomical for fingerprint identification. For this reason a survey was undertaken to investigate if fingerprints are indeed bandlimited, and if so, to establish an appropriate sampling rate.

4.3 Frequency Bandlimitations of Fingerprints.

In order to investigate the frequency content of fingerprints, ten fingerprints were selected at random from a file of prints, originally obtained from the R.C.M.P. Each of these prints was magnified approximately 10 times and the resulting photograph sampled at a high rate to minimize aliasing. The resulting array of samples was Fourier transformed by the FFT algorithm and the resulting frequency spectrum analyzed.

The sampling of the enlarged print was performed using an image conversion system belonging to the department of Computing Science. This system consists of a Sony DXC-2000A TV camera which scans the print, and a quantizer designed and built by Technical Services, University of Alberta. The quantizer samples the video output of the TV camera at instants that correspond to a regular grid of points on the fingerprints. The quantizer is connected to a PDP-9 computer which stores the samples from the quantizer on a magnetic disc. Also connected to the PDP-9 is a cathode ray tube display unit which allows a picture, stored in a sampled form on the disc, to be redisplayed and inspected.

The quantizer is capable of distinguishing between 64 levels of gray and the total field of view of the TV camera corresponds to 448x448 sampling points. Smaller areas can be selected with a corresponding reduction in the number of sampling points.

The time taken by the system to sample and store one picture is about 40 seconds. Thus the system is well suited for the processing of still pictures.

The samples of the prints were very closely spaced or over 20 samples per linear millimeter of the actual fingerprint (over 400 samples/mm^2). This very high rate of sampling was chosen in order to minimize aliasing so that it

could be neglected.

The array of samples obtained in this manner was then Fourier transformed using the FFT algorithm resulting in a frequency spectrum of each of the ten prints.

As was just mentioned, it was assumed that aliasing was negligible. This assumption was justified by the fact that the highest spectral components obtained were very small compared to the lower ones. The computed amplitude of these high components is the sum of the component in the fingerprint at that frequency and the amplitude which appears at that frequency because of aliasing. Since the total amplitude computed for high frequencies was low, certainly the amplitude appearing at these frequencies because of aliasing must have been low.

In order to give some representation of the bandlimitation of the prints, the total power contained within the frequency band $|u|<W$ and $|v|<W$ was calculated for several values of W. All 10 prints showed similar results, so only the two extremes are presented here.

Figures 12 and 13 show the two extreme cases. The print represented in Figure 12 is the print with the greatest concentration of power at low frequencies (i.e. the line plotted in Figures 12 and 13 rose fastest for this print) whereas the print represented in Figure 13 is the print out of the ten with the least concentration of power

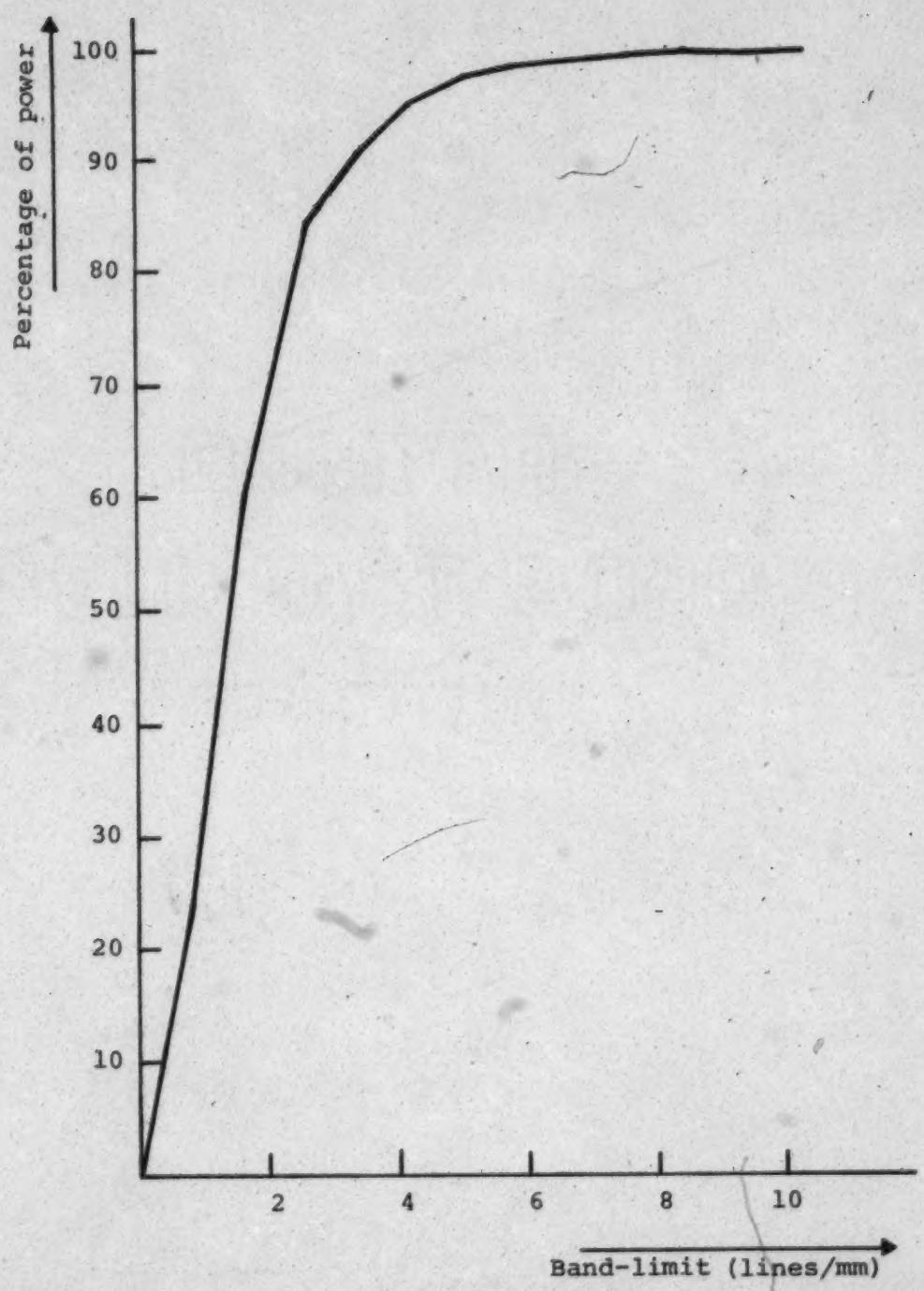

Figure 12. Percentage of total power as a function of band-limit. Low-frequency print.

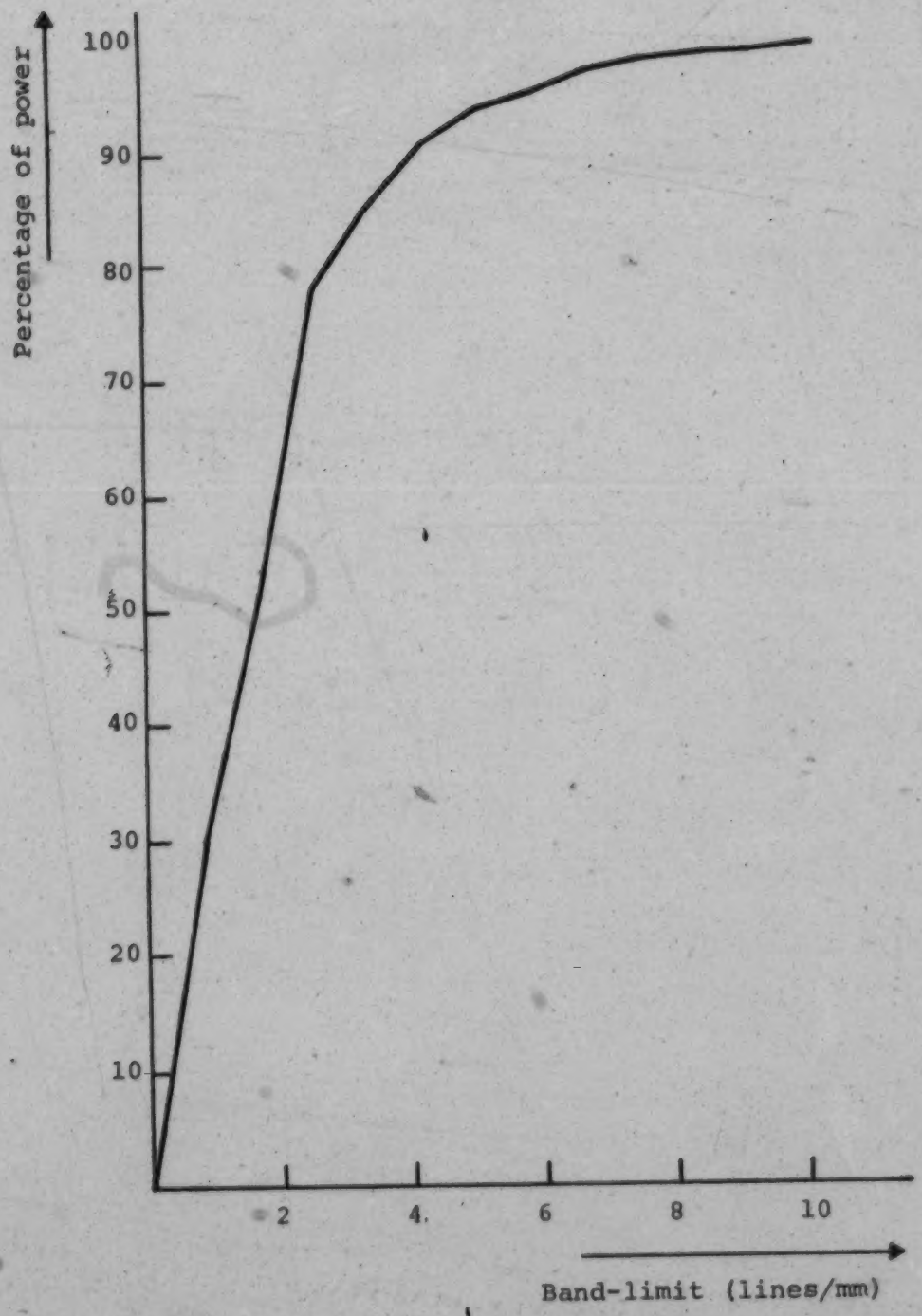

Figure 13. Percentage of total power as a function of band-limit. High-frequency print.

at low frequencies (the line in Figures 12 and 13 rose slowest for this print). From now on the former will be referred to as "the low-frequency print" and the latter as "the high-frequency print". From Figures 12 and 13 it is seen that the prints are indeed fairly well bandlimited. Even in the case of the high-frequency print, 90% of the total power of the print is contained at spatial frequencies lower than 4.2 lines/mm.

In selecting an appropriate sampling rate it should be kept in mind that the power at frequencies outside the band-limit W dictated by the sampling rate (c.f. equation (4.3)) will not only be neglected, but will in fact, through aliasing corrupt the frequency components within W. On the other hand it is desirable to keep the sampling rate down so that a large area of a fingerprint can be represented by a small number of samples.

With these criteria in mind it was decided that a sampling rate of 11 lines/mm (yielding a frequency band-limit of 5.5 lines/mm) was an appropriate compromise. Using this sampling rate, in the worst case (see Figure 13) only about 5% of the total power in a print is affected by aliasing and in the best case (see Figure 12) about 2.5% of the total power is affected. At this sampling rate 1.2x1.2 cm^2 of a fingerprint can be represented by 128x128 samples, and 256x256 samples would be sufficient to represent a complete fingerprint.

CHAPTER 5

PRODUCTION OF A LOHMAN FILTER

5.1 Data Collection

In Chapter 3 the theoretical basis of the Lohman filter was explained and in the last chapter it was described how a pattern can be sampled in order to obtain the data required to construct the filter. In this chapter the complete process of making a Lohman filter will be discussed.

Figure 14 shows a flow diagram of the operations required to produce a Lohman filter, starting with a photographic record of a fingerprint and finishing with a Lohman filter matched to that print.

The fingerprints used in the experiments were obtained as records on a microfilm. Thus the first step in the production of a Lohman filter is to enlarge the print whose filter is required onto photographic paper. The scale of the reproduction is determined by the image conversion system used to sample the prints and was in the present work approximately 10 times the natural size. This enlargement was performed by Photographic Services, University of Alberta, and was done by a two-step process.

The image conversion system used was described in the previous chapter and is drawn in a schematic form in

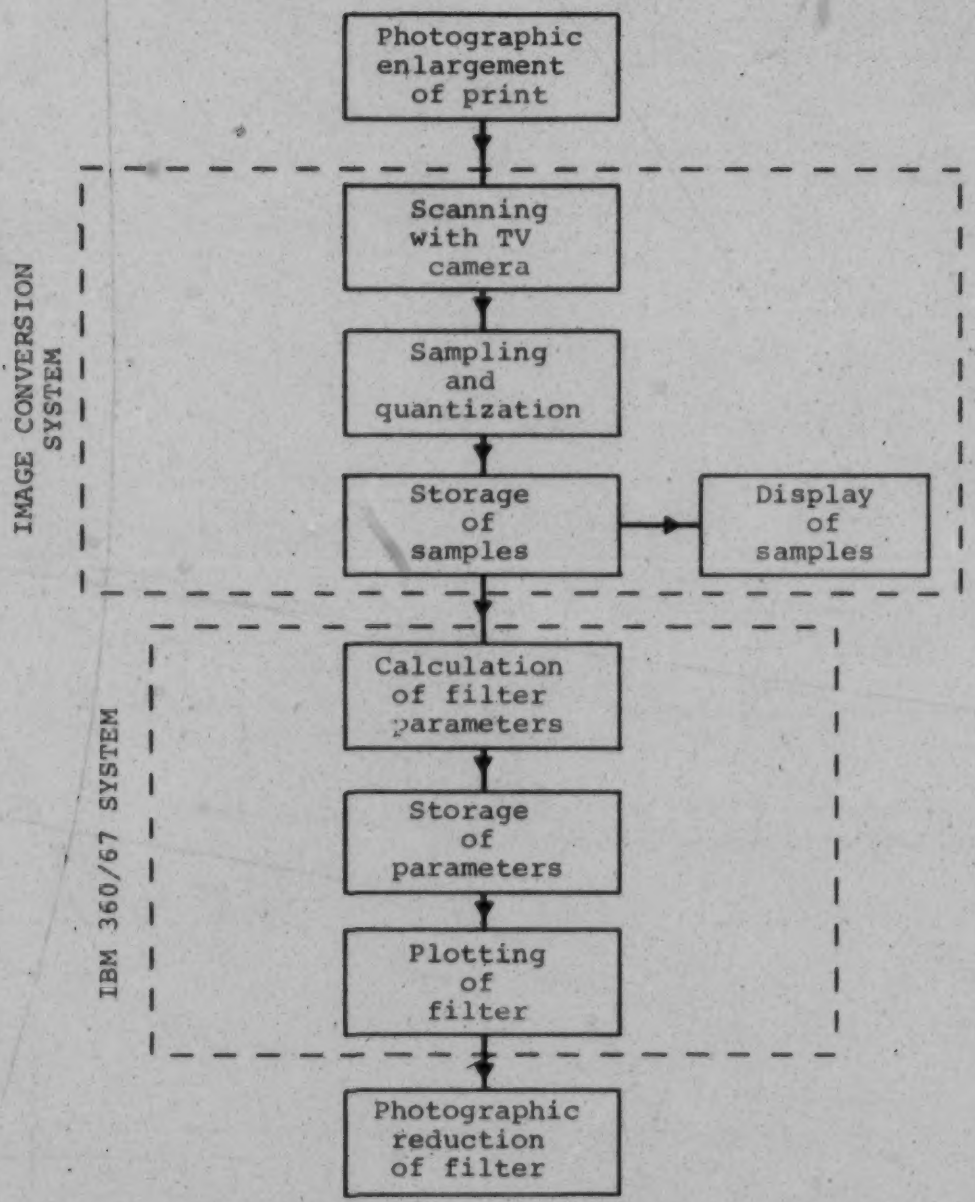

Figure 14. Production of a Lohman filter.

Figure 14. The image conversion system outputs an array of numbers describing the darkness of the print at points on a regular grid. In the experiments 128x128 samples were used and a sampling density of 5.5 samples/mm in the two perpendicular directions in the print plane was used.

The output used from the PDP-9 computer was in the form of punched paper tape and contained the data as a 128x128 (=16384) element vector of integers 0 to 63, corresponding to the 64 levels of gray distinguishable by the quantizer.

Unfortunately the computing system at the Department of Computing Services did not include a high speed paper tape reader at the time of the experiments. In order to input the data to the IBM 360/67 computer the paper tapes first had to be translated onto magnetic tape which could be read by the IBM 360/67. This translation was done in the Division of Biomedical Engineering, Clinical Sciences Building, University of Alberta, using their computing facilities. The translation is not indicated in the flow diagram in Figure 14.

5.2 Computing and Plotting

Once the array of samples has been stored in the IBM system it is required to evaluate the parameters describing a Lohman filter and then use the Calcomp 663 plotter to plot an enlarged version of the filter.

Two computer programs were written for this purpose. The first program uses the Fourier transforming subroutine HARM which is available in the IBM Scientific Subroutine Package to Fourier transform the array of samples obtained from the image conversion system. The elements of the Fourier transform are then converted to an amplitude and phase notation instead of the real and imaginary notation outputted from HARM. Finally, the amplitudes and phases are used to calculate the parameters of the filter according to equations (3.23) and (3.24). Both this program and the program used to create the plots are listed and explained in Appendix B.

As pointed out in Chapter 3 there are many shapes of apertures that fulfill the requirements placed on a Lohman filter. Referring to the notation of Figure 4 the shape of apertures used in the present filters was the same as drawn in Figure 4 except that W_{nm} was not varied but was taken as a constant equal to 1. Instead c was allowed to vary between 0 and 1/2 to determine the amplitude of light emerging from each cell. Thus each aperture extends over the whole cell in the v direction and the width in the u direction was varied from 0 to 1/2 the cell width. If an amplitude called for an aperture width of less than one stroke of the plotter pen, a single line was drawn and the length reduced appropriately. If the area of the required aperture was less than the pen tip no aperture was drawn.

As an indication that neglecting these small apertures was reasonable, it should be pointed out that the largest aperture neglected is only about 1/500th of the area of the largest aperture.

The plotting program listed and explained in Appendix B plots the filter column by column, decides for each cell which type of aperture is required and draws it according to the procedure described above. This plotprogram makes use of subroutine PLOT which is available in the Calcomp Subroutine Package.

The final step in the production of the filter is to photographically reduce the plot onto photographic film such that apertures drawn in black on the plot become transparent and the white background becomes opaque.

The scale used in the plotting was .22 inches/cell (.56 cm/cell) and this was reduced to a filter of size 100 microns/cell or a 55 times reduction. This reduction was again carried out by Photographic Services and was done in two steps.

5.3 Cost of a Filter.

In the last chapter the cost of computing and plotting was found to be about $20 for a 128x128 cell filter and about $85 for a 256x256 cell filter. Costs other than computing and plotting costs are the cost of sampling a picture, and that of the photographic processing. It is

difficult to assess the cost of sampling since in the present work the image conversion system was lent free of charge by the Department of Computing Science.

The cost of the photographic work involved, both the enlargement of the print and photoreduction of the plotted filter, was about $5-10 for each filter.

Thus the cost of a complete filter can be estimated as $25-30 for a 128x128 cell filter and about $95-100 for a 256x256 cell filter.

CHAPTER 6

EXPERIMENTS

6.1 Experimental Arrangement

In Chapter 2 spatial filtering is explained in terms of the optical system shown in Figure 1. This system can be used for any spatial filtering experiment and has the advantage that Fourier transforming properties of lenses can easily be explained in terms of this system. The system sketched in Figure 15 is, however, better suited for practical experimentation [23] as will be seen later and will be used in the experiments described in this chapter. The properties of this latter system are derived in detail in reference [23] and only the most important results will be mentioned here.

In order to obtain an exact Fourier transform of any object it must be placed one focal length in front of the Fourier transforming lens and then the exact Fourier transform appears in the back focal plane of the lens [14]. This is the arrangement used in the system shown in Figure 1.

If on the other hand, the object is placed behind the lens less than one focal length away, the Fourier transform of the object still appears in the back focal plane of the lens but this time it is multiplied by a spherical phase factor [14]. The filtering system drawn in

Figure 15 makes use of this arrangement of lens and object to perform the Fourier transformation.

Referring to Figure 15, L1 is the lens which performs the Fourier transformation and is illuminated by a plane wave. The object to be filtered is placed in plane P1 which may be moved along the optical axis of the system. As previously mentioned in this case the Fourier transform of the object which appears in plane P2, the back focal plane of lens L1, is multiplied by a spherical phase factor.

Using the notation of Chapter 2 and with reference to Figure 15, the spatial frequency coordinates, u and v in plane P2, are related to the real coordinates by

$$u=x/(\lambda D) \quad \text{and} \quad v=y/(\lambda D) \tag{6.1}$$

Comparing the above equation to equation (2.17) it is seen that they are the same except the focal length f in equation (2.17) is replaced by D, the distance between P1 and P2 in Figure 15. Since plane P1 can be moved along the optical axis, D is a variable and thus the scale of the transform in plane P2 is variable. This feature is one of the main advantages of the system shown in Figure 15 over the one in Figure 1 since it allows errors in scale of either the object or the filter to be compensated for by an appropriate choice of D.

Another advantage of the system in Figure 15 is that it is more compact since the Fourier transformation

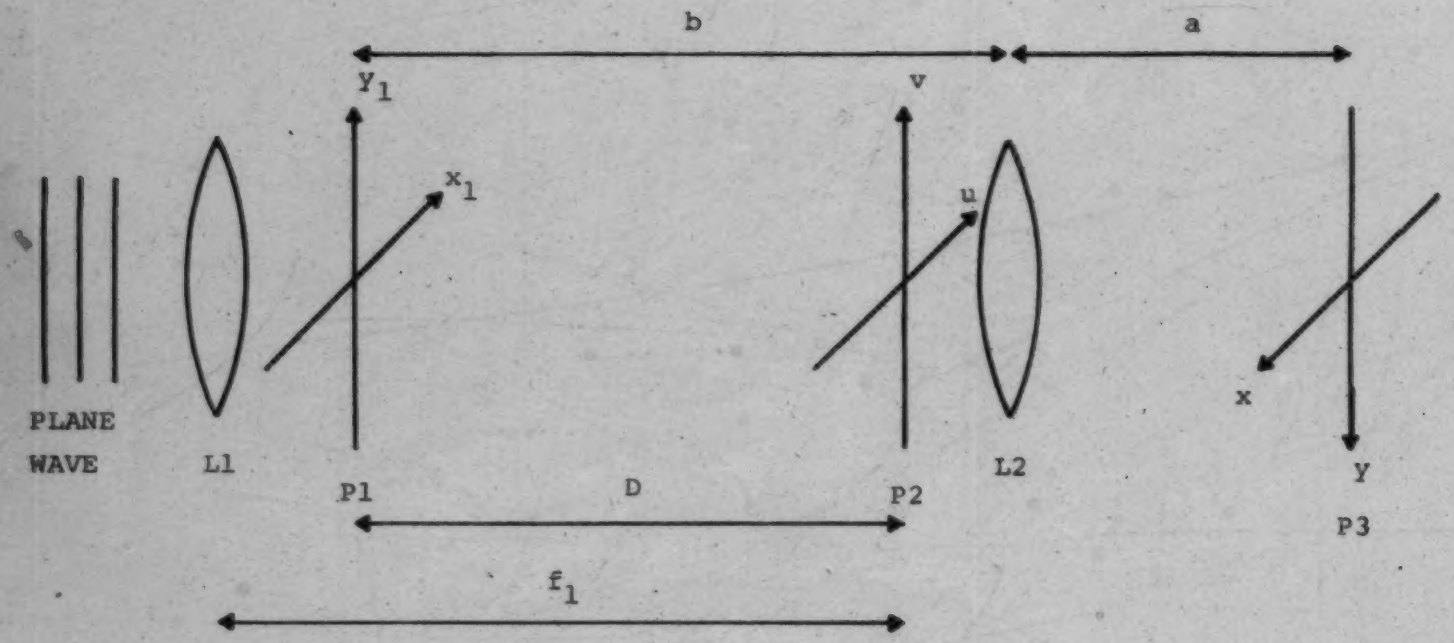

Figure 15. Optical filtering system used for experimentation.

only requires one focal length compared to two focal lengths required by the system of Figure 1.

Referring again to Figure 15, lens L2 images the filtered version of the pattern in plane P1 onto plane P3. In order that a focused image appears in plane P3 the relative positions of P1, L2 and P3 have to satisfy the well known imaging condition [14] which in terms of the parameters in Figure 15 can be written as

$$1/a + 1/b = 1/f_2 \qquad (6.2)$$

where f_2 is the focal length of lens L2.

6.2 Positioning Accuracy Required

It can be seen by inspection of equation (6.1) that the origin of the spatial frequency coordinates in plane P2 is defined by the optical axis and does not depend on the exact position of the object perpendicular to the optical axis in plane P1. The positioning of the object in this direction is therefore not very critical. It is only necessary that the object remains fully illuminated during the filtering experiment. However, as the object is moved in plane P1 (perpendicular to the optical axis), the filtered image also moves in plane P3. Thus in order to decide whether recognition has taken place or not the point of light indicating recognition must be searched for in plane P3.

It is, however, important that the filter is

accurately placed in plane P2. As previously mentioned the origin of the spatial frequency coordinates is the optical axis. In order that the filter matches the Fourier transform in plane P2, the point on the filter which corresponds to zero frequency on the Fourier transform of the object must be placed on the optical axis with sufficient accuracy.

In order to obtain some estimate of the accuracy required in the positioning of the filter perpendicular to the optical axis the following argument is adopted:

In the derivation of a Lohman filter it was assumed that the complex transmittance varies slowly within each cell. (This was the assumption which allowed the transmittance of each cell to be approximated by one aperture only.) If therefore the error in placement of the filter in plane P2 is small compared to the dimension of a cell, the resulting error in light transmitted through the filter can be expected to be small.

In the experiments performed all the filters consisted of 128x128 cells and had an overall size of 13x13 mm^2. Thus the side of each cell is approximately 0.1 mm or 100 microns.

Let the phrase "small compared to the dimension of a cell" mean "less than 1/10 the cell side". Then it can be estimated that it is necessary for recognition that the

filter deviates no more than 10 microns from its correct position.

Of course it is possible that the complex transmittance does not only vary slowly within each cell, it may vary slowly within several cells. If this was the case the above estimate of the accuracy to be achieved is a worst case estimate.

Vander Lught has published some theoretical studies about the detericration in signal to noise ratio as a function of the error in the placement of his filter [24]. These studies show that displacement of the filter in the axial direction is relatively unimportant so that the accuracy required can easily be achieved by manually sliding the filter holder along an optical bench.

In designing a holder for the filter the main criterion to be met was therefore that the filter could be positioned with an accuracy of at least 10 microns in the directions perpendicular to the optical axis.

6.3 Experimental Equipment

Referring once more to Figure 15, the plane wave used as illumination was derived from a Spectra Physics Stabilite Helium-Neon laser of wavelength :6328 micron and a Spectral Physics model 311 collimating lens assembly. The Fourier transforming lens L1 had a focal length of 152 cm and a diameter of 10.4 cm. The imaging lense L2 had a

focal length of 54 cm and a diameter 5.2 cm. The two lenses L1 and L2 were mounted on a heavy cast-iron optical bench together with a holder in plane P1 containing the object (fingerprint) and a holder in plane P2 for the filter. All the components on the optical bench could be slid along the bench and by means of a vernier positioned with a 0.2 mm accuracy.

Plane P3 contained a simple paper sheet to enable the inspection of the light distribution in the plane. All power measurements in plane P3 were performed by the use of a Spectra Physics model 401B power meter. In all cases the power was measured through a circular aperture of diameter approximately 1 mm.

The filter holder was made at the Machine Shop, Department of Electrical Engineering. Figure 16 illustrates the mechanical design used to achieve the required accuracy in positioning the filter. The outside frame is composed of two frames . Each frame is cut out of 3/4 inch sheet aluminium and groves are cut into the frames to accommodate the hardened ground steel rods shown in Figure 16. The sledge shown slides along the steel rods on precision low friction ball bushings arranged in the fashion indicated in Figure 16. In order to control the position of the sledge accurately a micrometer is mounted through the outside frame to push the sledge along. A steel spring holds the sledge against the micrometer.

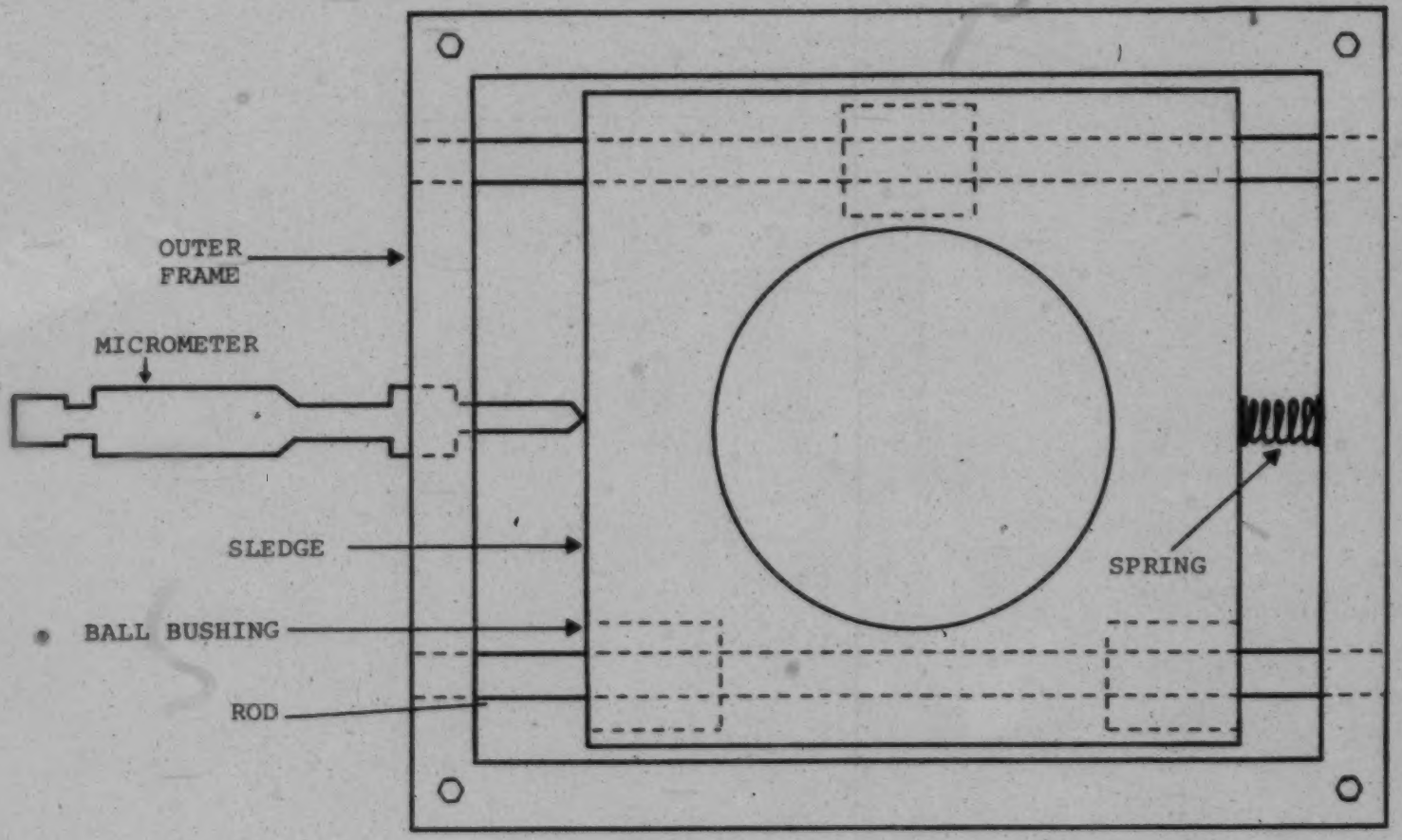

Figure 16. Mechanical design to position filter in u direction.

The micrometer is a 40 turns/inch micrometer which indicates that each turn of the micrometer shaft corresponds to a motion of the sledge of approximately 625 microns and ten microns correspond to 6 degrees of turning which is easily controlled.

Finally, in order to achieve the same accuracy of positioning in the other direction a similar device is mounted on the sledge, the orientation of the second device being perpendicular to the first one. The apertures on the two devices overlap to allow light to pass through. Now the filter can be mounted on the sledge of the second device, covering the circular openings of both sledges. The filter can be mounted with or without a liquid gate which will be described shortly.

When a Vander a Lught or a Lohman filter is said to affect only the amplitude of a light wave it is assumed that the photographic film used to record the filter is of uniform thickness. With commercially available films this is usually not the case and the variation in thickness of the film can give rise to errors in the phase distribution of a light wave emerging from the filter and reduce its performance [17]. In order to reduce the effect of thickness variation of the film the previously mentioned liquid gates are used.

A liquid gate consists of two highly polished

glass plates between which the film is inserted together with a small amount of oil with index of refraction as close as possible to that of the film. In this arrangement the oil fills the depressions in the film and the spatial variation in optical path length through the gate is small.

The glass plates used for the liquid gates were polished in the optics shop of this Department and dibutyl phtalate was used as index matching oil

As previously stated, liquid gates could be mounted on the filter holder and also on the holder which contained the object (fingerprint). The latter holder could also be tilted about the optical axis and the angular position set accurate to ±10 minutes. This enables the object to be adjusted in angular position to match the filter.

6.4 Experimental Results

The first experiment was designed to confirm and demonstrate the ability of the Lohman filter to recognize fingerprints.

Eight prints were selected from the file of prints acquired from the R.C.M.P. Of these eight prints three were used as originals to produce Lohman filters.

Each of these 3 filters was then used to detect the appropriate print from the selection of eight.

The prints were prepared in a form suitable for the experimental system described in the last section. A 1.2x1.2 cm^2 section of the print was made into a negative transparency of 0.8x0.8 cm^2. This particular reduction (33%) was chosen because it was convenient to work with in the system used. These transparencies were used as objects in the experiments and mounted in plane P1.

The filters were made by magnifying the appropriate object about 15 times (10 times the real size of a fingerprint) or to a size suitable for sampling by the image conversion system described in section 4.3. The 128x128 array of samples was Fourier transformed and a Lohman filter made using the programs and computing facilities described in Chapter 5.

Each of the 3 filters was then tested by the following method:

Both the filter and the object which it was known to match were mounted in liquid gates and inserted into their holders. The light intensity distribution in plane P3 was observed and the position of the filter adjusted by use of the micrometers on the filter holder, and by sliding the holder along the optical bench, until a recognition spot was found. The system was then further adjusted so as to maximize the power in the recognition spot. After these adjustments the system is known to be correctly set for identification of prints prepared in the fashion described

earlier. (The system is set for the correct scale of objects and the zero frequency in the filter is at the optical axis.)

Now the print in plane P1 was replaced by one of the other eight and a recognition spot visually searched for in plane P3. If a recognition spot was found its power was measured but otherwise the power in plane P3 where the recognition spot should have appeared was measured. This was repeated for all the eight prints, ending with the one the filter was known to match.

The results of these experiments are shown in tables 1,2 and 3. The tables indicate for each filter and each object whether a recognition spot was observed in plane P3 and the power in plane P3 at the location where the recognition spot should have appeared. In each table the power has been normalized to the power of the recognition spot.

From the tables it is seen that a recognition spot is visually observed only when the object is the print to which the filter is matched. The maximum power in the location of the recognition spot when the filter does not match is only 14% of the power measured when matching to the filter occurs.

Next the effect of a small displacement of the filter in a direction normal to the optical axis was

OBJECT NO.	RECOGNITION SPOT OBSERVED	POWER IN PLANE P3
1	YES	1.00
2	NO	0.05
3	NO	0.04
4	NO	0.05
5	NO	0.08
6	NO	0.04
7	NO	0.10
8	NO	0.07

TABLE 1. RESULTS OF FINGERPRINT RECOGNITION EXPERIMENT. FILTER MATCHED TO OBJECT NO. 1.

OBJECT NO.	RECOGNITION SPOT OBSERVED	POWER IN PLANE P3
1	NO	0.14
2	YES	1.00
3	NO	0.04
4	NO	0.06
5	NO	0.06
6	NO	0.02
7	NO	0.06
8	NO	0.04

TABLE 2. RESULTS OF FINGERPRINT RECOGNITION EXPERIMENT. FILTER MATCHED TO OBJECT NO. 2.

OBJECT NO.	RECOGNITION SPOT OBSERVED	POWER IN PLANE P3
1	NO	0.07
2	NO	0.05
3	YES	1.00
4	NO	0.10
5	NO	0.03
6	NO	0.08
7	NO	0.04
8	NO	0.12

TABLE 3. RESULTS OF FINGERPRINT RECOGNITION EXPERIMENT. FILTER MATCHED TO OBJECT NO. 3.

studied. The filters were first adjusted to maximize the power in the recognition spot and then deliberately moved from their correct position in both the positive and negative x and y directions. The reduction in power in the recognition spot was recorded as a function of the displacement. Figure 17 shows a typical result.

From Figure 17 it is seen that the power in the recognition spot drops by 10% if the position of the filter is incorrect by approximately ±75 microns. Thus the estimates of the accuracy required in positioning presented in section 6.2 are seen to be too stringent. This could have been expected since the estimate applied to the worst case.

The effect of angular displacement of the filter from its correct position was also studied. In these experiments the object holder was used to initially adjust the relative angular position of print and filter to maximize the power in the recognition spot. Then the angular position of the print was changed in both the clockwise and counterclockwise directions and the power in the recognition spot recorded as a function of the angular position.

Figure 18 shows a typical set of these measurements. If a power loss of 10% is once more taken as a criterion, it is seen from Figure 18 that the accuracy of positioning in the angular direction has to be better than

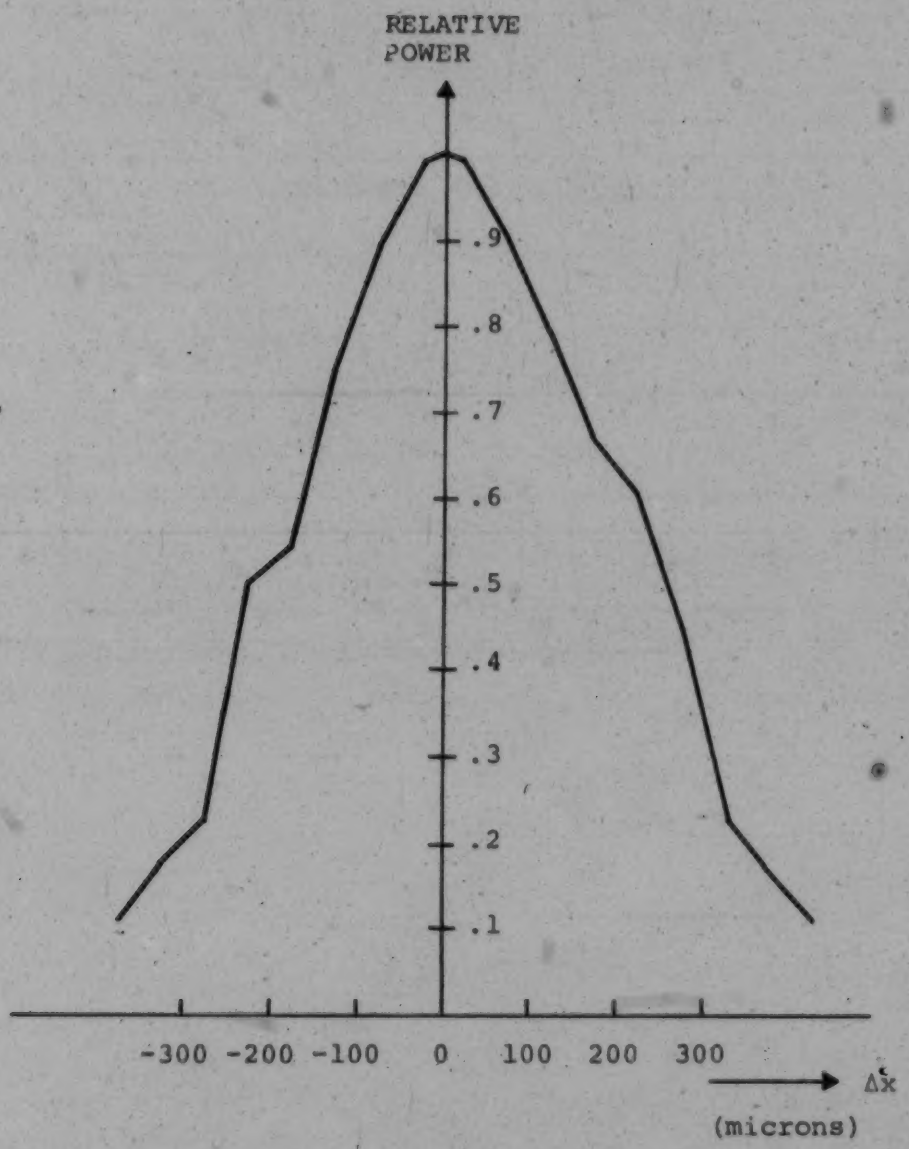

Figure 17. Power in the recognition spot as a function of placement error perpendicular to optical axis.

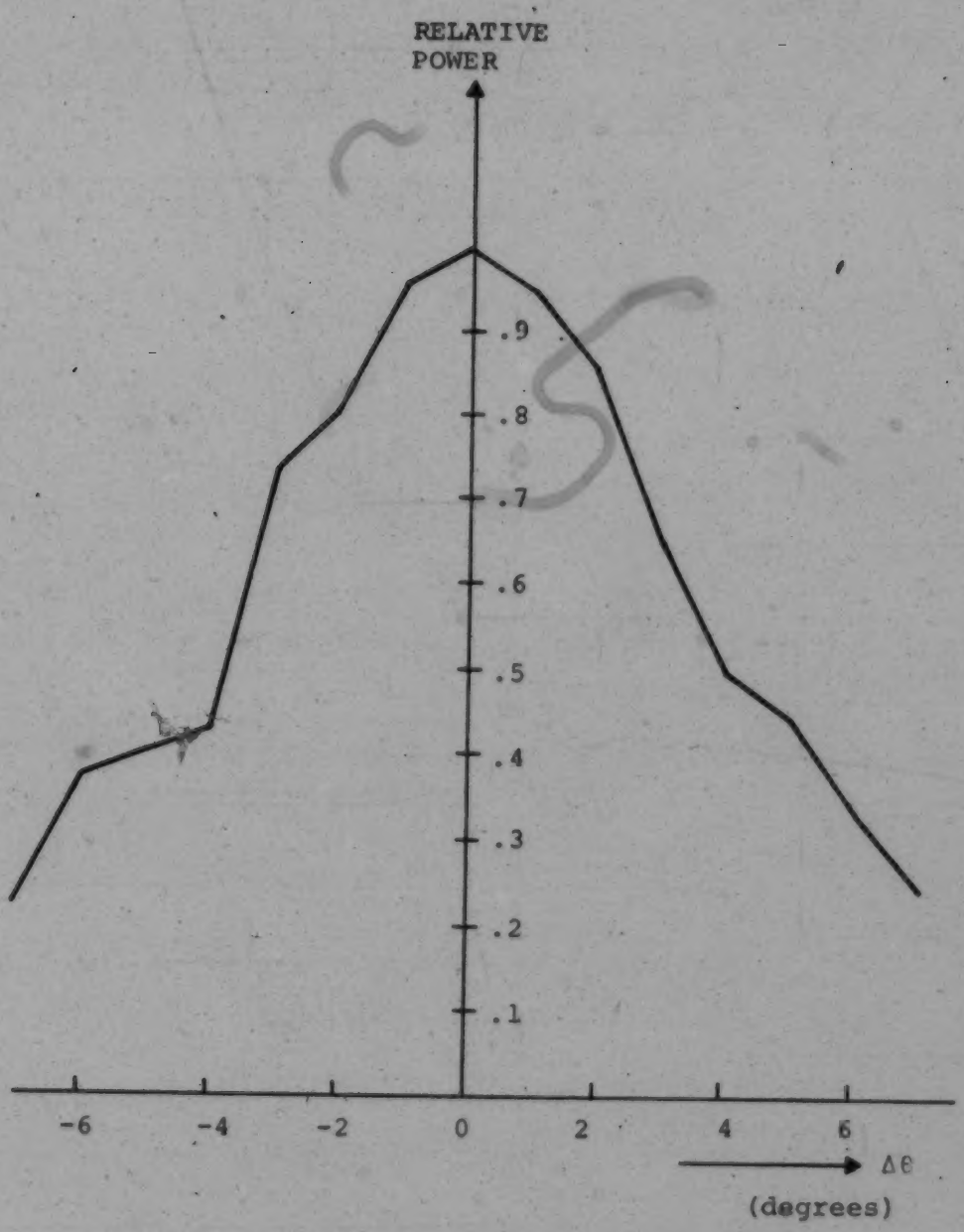

Figure 18. Power in the recognition spot as a function of error in angular position.

approximately ±1.5 degrees. This result may be compared with reference [5] where it is stated that recognition takes place if the positioning of a Vander Lught filter is accurate to ±3 degrees. In the present experiments a recognition spot was observed when the angular position of the filter was inaccurate by ±3 degrees but its power was only 65-75% of maximum.

Finally, it should be mentioned that throughout the experiments an improvement was observed due to the use of a liquid gate for the objects. The objects were used many times for different experiments and after each use they were washed in detergent to remove any oil left from the use. In the first experiments it was found that the power in the recognition spot decreased by about 20% when a liquid gate was not used. It was found, however, that this percentage slowly increased as the experiments progressed and reached 40-45% at the end of the experiments. The reason for this phenomenon is very likely that small scratches and imperpections develop as the objects are used and washed, reducing the efficiency of the object. This reduction in efficiency could be quite serious in a practical application if liquid gates are not used since a 20% reduction may possibly be tolerable but not 40-45%.

6.5 Discussion

The first set of experiments demonstrate convincingly the ability of the Lohman filter to identify

fingerprints. For each of the three filters a visual inspection left no doubt that the print which the filter was matched to was the only print which caused a recognition spot to appear in plane P3. The power measurements substantiate the above statement but it should be pointed out that the power measurements do not really tell the full story. When matching did not occur the light distribution in plane P3 was fairly slowly varying whereas a sharp point of light was observed when matching occurred.

The results of this experiment may be compared with the results mentioned in the introduction where 64 Vander Lught filters were tested with a file of 10,000 prints. Since in 65% of the cases the Vander Lught filter identified the correct print alone out of 10,000, it can be seen that while the present experiments confirm the ability of the Lohman filter to identify fingerprints,no specific conclusions as to its capability for prescreening a larger number of fingerprints can be reached from the small number of measurements.

The only way to settle the above problem is to develcp criteria in terms of power in plane P3 and the appearance of a recognition spot. These criteria would have to be based on a larger number of experiments.

The positioning of the filter in its plane is one of the aspects of optical filtering which frequently causes concern. The experimental results typified by Figure 17

show that the positioning accuracy required for the present experiments is easily achieved.

The experimental system described can be used to process more than one print at the same time. If an array of prints, each prepared in the way previously described is presented as an object and one of these prints matches the filter then the location of the recognition spot tells which of the prints matches the filter (the location of the recognition spot moves as the correct print is moved in plane P1).

As the number of prints processed in parallel increases, the accuracy required in positioning increases. The reason for this is that while each print in the input has the same bandwidth the spatial extent increases. The "space-bandwidth product" (SB product) is a measure of the total amount of information contained in the object. All the information in the object is also contained in its Fourier transform. The overall size of the Fourier transform of the object does not increase as the SB product increases. So, to accommodate the increased information, the structure of the Fourier transform becomes finer and thus positioning becomes more critical.

It is fcund experimentally that with the present system the filter can be positioned seven times more accurately than is required for one print. Thus if only the cross section of the laser beam is expanded the system

is capable of processing 49 (7x7) prints in parallel.

The experiments with angular positioning show that in order to maintain 90% of the maximum power in the recognition spot the angular positioning accuracy must be approximately ±1.5 degrees.

When a fingerprint is found at the scene of a crime the police are generally able to pinpoint its orientation tc ±15 degrees [25]. Thus for the purposes of criminal investigation a print would have to be tried at 10 different angular positicns in order to process it completely. This could be done by constructing 10 different filters and processing the print sequentially by these 10 filters in separate systems or separate branches of the same machine. Alternatively the parallel processing capability of the filtering system could be used to this end.

The aspect of the experimental results which are likely to cause the most difficulty in practical use is the dependance on a liquid gate to insert the object into in order to achieve consistent and accurate measurements. To mount each object of a large collection in a liquid gate is unpractical and to mount each object just prior to measurement is time consuming.

When the objects were new and unworn the power in the recognitien spot was found to decrease by about 20% when

a liquid gate was not used for the object. However, a recognition spot was still observed. Thus it may be possible to do without a liqiud gate and obtain useful results.

It appears that in order to increase the useful life of an object other cleaning methods or alternatively, better recording materials than the photographic film have to be developed.

CHAPTER 7

SUMMARY AND CONCLUSIONS

In recent years optical spatial filtering and in particular optical matched filtering has found many practical applications and the interest in this field has been considerable.

A convenient way of producing filters capable of controlling the spatial distribution of both amplitude and phase of light transmitted through them was for a long time the main obstacle in the field of matched filtering. This problem has been greatly reduced in recent years by the development of methods to produce a special type of holograms or masks, consisting of absorption patterns only which can be used as matched filters.

The first of these methods is an optical (interferometric) method due to A. Vander Lught. Many experiments, some of which are mentioned in the introduction, have been carried out using filters produced by this method and the potential and limitations of these filters are well documented.

A second method of producing matched filters is due to A. W. Lohman. This method employs a digital computer and a computer guided plotter to produce a filter

from a mathematical knowledge of the filtering operation.

In many applications a Vander Lught filter can be very easily produced. For this reason less attention has been paid to matched filters produced by Lohman's method than to the Vander Lught filters and no study of the performance of the Lohman filters as matched filters has been published.

While the methcd of production is quite different for the two filters, they appear to have many properties in common. However, no study of these similarities of the two filters has been published.

In this thesis a theoretical study of the transmission properties of the two filters has been carried out and it has been shown that the transmission functions of the two filters are indeed very similar. The similarity is so strong that the Lohman filter can be regarded as a computed binary simulation of the Vander Lught filter.

The above theoretical studies indicated that in most filtering problems either a Vander Lught or a Lohman filter could be used. The choice as to which filter is used would depend mainly on the ease and economy of production. There are, however, many instances where the use of a Lohman filter is advantageous or a Lohman filter can more easily be produced than a Vander Lught filter.

In order to study experimentally some of the

properties of Lohman filters, fingerprints have been used as test patterns in the present studies. Initially a survey was carried out to determine the sampling density required from a fingerprint to compute a Lohman filter. It was shown that a sampling rate of 5.5 samples/mm was sufficient and thus a complete fingerprint can be represented by 256x256 samples. In this connection the cost of producing a Lohman filter has been outlined and it was found that the cost of producing a typical filter consisting of 128x128 elements is approximately $25-30. Using the sampling rate previously determined, some filters of fingerprints were made according to the Lohman method. These filters were experimentally tested to study their properties and the practical difficulties in their application to fingerprint identification. The first experiment performed with these filters was designed to test the ability of the filters to identify fingerprints. In the experiment each of three filters was used to identify one print from a collection of eight. The results of the experiment were very encouraging since in all cases a sharp recognition spot was observed when the print which the filter was designed to detect was being considered. No other print caused a visual recognition spot and the maximum power measured where the recognition spot should have appeared was only 14% of the power measured when recognition took place. Experiments were next performed to investigate the requirements of the experimental system. It was found that in order to obtain

good results in the recognition experiment the filter had to be accurately positioned in the appropriate plane of the recognition system. The accuracy required in the positioning normal to the optical axis of the system was found to be ±75 microns while it was found that the filter and object had to be adjusted to within ±1.5 degrees in the relative angular position.

The experimental system used could be adjusted to ±10 microns normal to the optical axis and an angular position of ±10 minutes. Thus the accuracy required is easily achieved. It should in fact be possible to design a device to automatically change the filter and position it with the required accuracy.

It was shown that the experimental system is capable of processing many prints in parallel and with the achievable accuracy in the present system up to 49 prints can be processed at the same time.

The experimental result which was found to potentially cause the most difficulty was that during the experiments the filter and preferably also the object had to be mounted in liquid gates.

It was found that if a liquid gate was not used, the efficiency of the recognition process decreased 20-45% depending on the conditicn of the object.

In many applications, for example, in fingerprint

identification it may be possible to tolerate a 20% drop in efficiency if other checks, such as human observation, are increased. However, a 45% drop in efficiency would in most applications be excessive.

Since the mounting of a large collection of fingerprints in liquid gates would be exceedingly cumbersome and expensive the use of liquid gates similar to the ones used in the present experiments would be disadvantageous. It would therefore be important to develop recording materials which do not require the use of liquid gates. Alternatively, it might be possible to design more convenient liquid gates and develop methods for preserving the object in a good condition despite repeated use.

Finally it may be pointed out that while the requirement of liquid gates might be a serious limitation due to the large number of objects that would likely have to be tested, there are many applications for Lohman filters where the speed with which the object (and/or filter) can be changed is not critical.

REFERENCES

[1] G. W. Stroke, "Optical computing," IEEE Spectrum, December 1972.

[2] W. M. Brown, "Analysis of linear invariant systems," Chapter 9, McGraw-Hill Book Company 1963.

[3] A. B. Vander Lught, "Signal detection by complex spatial filtering," IEEE Transactions on Information Theory IT10:2, pp. 139-145 (1964).

[4] A. B. Vander Lught, F. B. Rotz and A. Klooster Jr., "Character reading by optical spatial filtering," Optical and Electro-optical Information Processing, p. 125, M.I.T. Press 1965.

[5] V. V. Horvath, J. M. Holeman and C. G. Lemmond, "Holographic technique recognizes fingerprints," Laser Focus, June 1967.

[6] J. Tsujiuchi, K. Matsuda, N. Takeya, "Correlation techniques by holography and its application to fingerprint identification," Applications of Holography, p. 247, Plenum Press 1971.

[7] M. Eleccion, "Automatic fingerprint identification," IEEE Spectrum, September 1973.

[8] B. R. Brown and A. W. Lohman, "Complex spatial filtering with binary masks," Applied Optics, vol. 5, pp. 967-969 (1966).

[9] A. W. Lohman and D. P. Paris, "Binary Fraunhofer holograms generated by computer," Applied Optics, vol. 6, pp. 1739-1748 (1967).

[10] A. W. Lohman, D. P. Paris and H. W. Werlich, "A computer generated spatial filter applied to code translation," Applied Optics, vol. 6, pp. 1139-1141 (1967).

[11] A. W. Lohman and D. P. Paris, "Computer generated spatial filter for coherent optical data processing," Applied Optics, vol. 7, pp. 651-655 (1968).

[12] J. Kuhn and A. Fercher, Carl Zeiss Co. Obercochen, "Ein Holographischer Foucault-Test mit synthetischem Hologramm," (A holographic Foucault-test using a synthetic hologram). German Optical Society annual meeting 1971, Celle, W-Germany.

[13] J. W. Goodman, "Introduction to Fourier optics," Appendix, McGraw Hill Book Company 1968.

[14] Reference [13] Chapter 5.

[15] R. Bracewell, "The Fourier transform and its applications," Chapter 2, McGraw-Hill Book Company 1965.

[16] A. B. Vander Lught, "Practical considerations for the use of spatial carrier-frequency filters," Applied Optics, vol. 5, pp. 1760-1764 (1966).

[17] Reference [13] Chapter 7.

[18] A. B. Carlson, "Communication systems: an introduction to signals and noise in electrical communication," Chapter 2, McGraw-Hill Book Company 1968.

[19] J. W. Ccoley and J. W. Tukey, "An algorithm for the machine calculation of complex Fourier series," Mathematics of Computation, vol. 19, pp. 297-301 (1965).

[20] B. R. Brown and A. W. Lohman, "Computer-generated binary holograms," IBM Journal of Research and Developement, pp. 160-168, March 1967.

[21] W. T. Cochran et. al. "What is the fast Fourier transform," IEEE Transactions on Audio and Electroacoustics, vcl. AU 15, p. 45, June 1967.

[22] Reference [13] Chapter 2.

[23] A. B. Vander Lught, "Operational notation for the analysis of optical data-processing systems," Proceedings of the IEEE, vol. 5, pp. 1055-1063 (1966).

[24] A. B. Vander Lught, "The effects of small displacements of spatial filters," Applied Optics, vol. 6, pp. 1221-1225 (1967).

[25] K. V. Leung, Department of Computing Science, University of Alberta, Private communication.

APPENDIX A

DERIVATION OF EQUATION (3.12)

It is required to evaluate the inverse Fourier transform of equation (3.11) which is reproduced here for reference.

$$b(x,y) = F^{-1}\left\{ \sum_n \sum_m \text{Rect}\left[\frac{u-(n+P_{nm})\,d}{cd}\right] \text{Rect}\left[\frac{v-md}{W_{nm}d}\right] \text{Exp}(j2\pi x_o u)\right\} \tag{3.11}$$

The inverse Fourier transform of equation (3.11) can be obtained by Fourier transforming equation (3.11) and then changing the signs of the coordinates in the Fourier plane. In Figure 5 the coordinates in plane P3 are negated with respect to the coordinates in plane P2 so that a direct Fourier transform expressed in the reflected coordinates is in fact the inverse Fourier transform (c.f. section 2.3). It is seen that the expression under the summation signs in equation (3.11) can be written as a product of two functions, one depending on u only and the other depending on v only. Thus the evaluation of the Fourier transform of equation (3.11) is reduced to evaluating the following transforms:

$$r(x) = F\left\{\text{Rect}\left[\frac{u-(n+P_{nm})\,d}{cd}\right] \text{Exp}\{j2\pi x_o u\}\right\} \tag{A.1}$$

and

$$t(y)=F\left\{\text{Rect}\left[\frac{v-md}{w_{nm}d}\right]\right\} \tag{A.2}$$

In order to evaluate the above equations the shift and similarity theorems of Fourier transforms are used. These theorems are stated below in terms of the coordinates in equations (A.1) and (A.2) but a proof can be found in reference [13].

Shift Theorem:

If G(u) is a complex function such that $F\{G(u)\}=g(x)$ and a is a complex constant then

$$F\{G(u-a)\}=g(x)\,\text{Exp}\{-j2\pi xa\} \tag{A.3}$$

Similarity Theorem:

If G(u) is as defined above and b is a complex constant then

$$F\{G(u/b)\}=|b|\times g(bx) \tag{A.4}$$

Finally, the Fourier transform of a Rect-function is required. This is given by [22]

$$F\{\text{Rect}(u)\}=\text{Sinc}(x) \tag{A.4}$$

Combining equations (A.5) and (A.4) and changing variables yields

$$F\{\text{Rect}(u/b)\}=|b|\times\text{Sinc}(bx)=|b|\times\text{Sinc}(t) \tag{A.6}$$

where t=bx. Now the shift theorem and (A.6) can be combined which with resubstitution for t results in

$$F\{\text{Rect}(u/b-a/b)=|b|\times\text{Sinc}(t)\,\text{Exp}\{-j2\pi ta/b\}$$

$$=|b|\times\text{Sinc}(bx)\,\text{Exp}\{-j2\pi ax\} \qquad (A.7)$$

This last equation can be used to solve (A.1) and (A.2). Consider first (A.1). In equation (A.7) let $a=(n+P_{nm}d)$ and let $b=cd$. With these values of a and b equation (A.7) gives the Fourier transform of the Rect-function in (A.1). Applying the shift theorem once more to allow for the exponential factor in (A.1) results in

$$r(x)=cd\,\text{Sinc}[cd(x+x_o)]\,\text{Exp}\{-j2\pi d(n+P_{nm})(x+x_o)\} \qquad (A.8)$$

Next in order to solve (A.2) let $a=md$ and $b=W_{nm}d$ in equation (A.7). This gives the direct result

$$t(y)=dW_{nm}\text{Sinc}(yW_{nm}d) \qquad (A.9)$$

Now in order to find the Fourier transform of the sum of products of Rect-functions in equation (3.11) the contribution due to the various Rect-functions is summed. This results in equation (3.12)

$$b(x,y)=cd^2\text{Sinc}[(x+x_o)cd]\times$$

$$\sum_n\sum_m W_{nm}\text{Sinc}(yW_{nm}d)\,\text{Exp}\{-j2\pi d[(n+P_{nm})(x+x_o)+my]\} \qquad (3.12)$$

APPENDIX B

COMPUTER PROGRAMS

The computational task involved in the production of Lohman filters is conveniently split in two. First the computation of the parameters which describe the filter and secondly the plotting of the filter.

Programs which perform these tasks are listed on the following pages. Comment statements have been extensively used so that the programs may be easily understood in context with the discussions in the main body of the thesis. Subroutines used in the main programs are listed immediately following the main program, except the system subroutines READ and WRITE and the Fourier transforming subroutine HARM. This last subroutine is available in the IBM Scientific Subroutine Package which is stored in the public file *SSPLIB in the computing system at Computing Services, University of Alberta. Subroutine PLOT is in the IBM Calcomp Subroutine Package stored in the public file *PLOTLIB.

PROGRAM TO CALCULATE FILTER PARAMETERS

```
C
C     THE FOLLOWING IS A FORTRAN SOURCE PROGRAM TO FOURIER
C     TRANSFORM AN ARRAY OF NUMERICAL PICTURE SAMPLES AND
C     COMPUTE THE PARAMETERS WHICH DESCRIBE A LOHMAN FILTER
C
      DIMENSION A(256,128),M(3),INV(4096),S(4096),VA(32768)
      INTEGER*2 VP(16384),LEN
      COMPLEX CA(128,128),C(64,64),CMPLX
      EQUIVALENCE (VA,CA),(VA,A)
C
C     READ INPUT DATA FROM A FILE
C
      DO 77 I=1,128
      K=(I-1)*128+1
   77 CALL READ(VP(K),LEN,0,LNR,1)
C
C     THE INPUT FILE CONTAINS INTEGERS 0 TO 63, CONVERT
C     THESE TO REALS 0.0 TO 1.0 AND EQATE TO THE REAL PART
C     OF THE COMPLEX NUMBERS TO BE INPUTTED TO HARM.
C
      DO 10 I=1,16384
   10 VA(2*I-1)=FLOAT(VP(I))/63.
C
C     SET INPUT PARAMETERS FOR SUBROUTINES HARM AND SFLE
C
      N1=128
      N2=128
      M1=64
      M2=64
      M(1)=7
      M(2)=7
      M(3)=0
C
C     REARRANGE INPUT FILE TO A SUITABLE FORM FOR HARM, CALL
C     HARM TO PERFORM FOURIER TRANSFORMATION AND REARRANGE
C     OUTPUT FILE
C
      CALL SFLE(CA,N1,N2,M1,M2,C)
      CALL HARM(A,M,INV,S,1,IFERR)
      CALL SFLE(CA,N1,N2,M1,M2,C)
C
C     CONVERT THE REAL AND IMAGINARY PARTS OUTPUTTED FROM
C     HARM TO AMPLITUDE AND PHASE NOTATION MAKING SURE THAT
C     IF BOTH REAL AND IMAGINARY PARTS ARE ZERO, CONVERSION
C     IS NOT ATTEMPTED AND AMPLITUDE SET TO ZERO.
C
      PI =3.14159
      DO 21 I=1,128
      DO 21 J=1,128
      RP=REAL(CA(I,J))
      CP=AIMAG(CA(I,J))
```

```
      IF(RP.EQ.0..AND.CP.EQ.0.)GO TO 21
      AMP=CABS(CA(I,J))
      PHASE=ATAN2(CP,RP)/(2.*PI)
C
C     THE ABOVE STATEMENT NORMALIZES THE PHASE TO VALUES
C     BETWEEN -1/2 AND 1/2. K IN EQN. (3.23) HAS BEEN
C     TAKEN AS 1.0.
C     NEXT STORE AMPLITUDE AND PHASE IN CA(I,J) AND GO
C     BACK TO CONVERT NEXT NUMBER.
C
      CA(I,J)=CMPLX(AMP,PHASE)
   21 CONTINUE
C
C     NEXT NORMALISE AMPLITUDES TO VALUES LT.OR.EQ. 1.0, BY
C     FINDING THE LARGEST AND DEVIDING ALL BY THAT VALUE.
C
      BIGAMP=0.
      DO 22 I=1,128
      DO 22 J=1,128
   22 IF(REAL(CA(I,J).GT.BIGAMP)BIGAMP=REAL(CA(I,J))
      DO 23 I=1,128
      DO 23 J=1,128
   23 CA(I,J)=CMPLX(REAL(CA(I,J)/BIGAMP,AIMAG(CA(I,J)))
C
C     FINALLY STORE THE PARAMETERS IN A FILE WHERE THEY CAN
C     BE USED BY THE PLOTTING PROGRAM.
C
      LEN=4096
      do 20 j=1,32
      K=(J-1)*1024+1
   20 CALL WRITE(VA(K),LEN,0,LNR,2)
      STOP
      END
C
C     SUBROUTINE SPLE INTERCHANGES 1ST AND 3RD QUADRANT AND
C     2ND AND 4TH QUADRANTS OF THE INPUT/OUTPUT MATRIX OF
C     SUBROUTINE HARM
C
      SUBROUTINE SPLE(CA,N1,N2,M1,M2,C)
      COMPLEX CA(N1,N2),C(M1,M2)
C
C     STORE 2ND QUADRANT IN C(I,J)
C
      DO 1 I=1,M1
      DO 1 J=1,M2
    1 C(I,J)=CA(I,J)
C
C     MOVE 4TH QUADRANT INTO 2ND QUADRANT
C
      DO 2 I=1,M1
      DO 2 J=1,M2
    2 CA(I,J)=CA(I+M1,J+M2)
C
C     MOVE C(I,J) INTO 4TH QUADRANT
```

```
C
      DO 3 I=1,M1
      DO 3 J=1,M2
    3 CA(I+M1,J+M2)=C(I,J)
C
C     STORE 1ST QUADRANT IN C(I,J)
C
      DO 4 I=1,M1
      DO 4 J=1,M2
    4 C(I,J)=CA(I,J+M2)
C
C     MOVE 3RD QUADRANT INTO 1ST QUADRANT
C
      DO 5 I=1,M1
      DO 5 J=1,M2
    5 CA(I,J+M2)=CA(I+M1,J)
      DO 6 I=1,M1
      DO 6 J=1,M2
    6 CA(I+M1,J)=C(I,J)
      RETURN
      END
```

PLOTPROGRAM

```
C
C     THE FOLLOWING IS A PROGRAM TO PLOT THE ENLARGED
C     ORIGINAL OF A LOHMAN FILTER. THE PROGRAM MAKES USE OF
C     ONE SUBROUTINE, PLCI
C
      DIMENSION VA(32768),WORK(2048)
      COMPLEX CA(128,128)
      INTEGER*2 LEN
      EQUIVALENCE (VA,CA)
C
C     SET THE SIZE OF EACH CELL (DIMENSION OF CELL= U X U)
C     AND THE THICKNESS OF PEN TO BE USED FOR PLOTTING
C
      U=.22
      PEN=.014
C
C     READ FILTER PARAMETERS FROM FILE WRITTEN BY
C     PROGRAM PREVIOUSLY LISTED AND SCALE THE AMPLITUDES
C     IF REQUIRED
      RMULT=4.
      CHOP=2.
      DO 88 I=1,32767,2
      VA(I)=VA(I)*RMULT
   88 IF(VA(I).GT.CHOP)VA(I)=CHOP
C
C     INITIALISE PLOTROUTINES AT A LOW ADDRESS IN CORE AND
C     SET ORIGIN AT TOP LEFT HAND CORNER OF FILTER, ALLOWING
C     FOR A .5 INCH MARGIN.
C
      CALL PLOTS(WORK,8192)
      CALL PLOT(.5,128.*U,-3)
C
C     INITIALISE A COUNTER FOR THE COLUMNS PLOTTED AND SX, TH
C     DISPLACEMENT FROM THE ORIGIN IN THE X-DIRECTION OF THE
C     LEFT TOP CORNER OF THE CELL TO BE PLOTTED.  THEN PLOT
C     THE FIRST COLUMN.  SUBROUTINE PLCL PLOTS THE APERTURE
C     WHEN GIVEN (SX,SY), THE COORDINATE OF THE TOP LEFT
C     CORNER OF THE CELL AND THE AMPLITUDE AND PHASE
C     PARAMETERS
C
    9 J=J+1
      SX=SX+U
      DO 10 I=1,128
      SY=-FLOAT(I)*U
      AMP=REAL(CA(I,J))
      PHASE=AIMAG(CA(I,J))
      CALL PLCL(SX,SY,AMP,PHASE,U,PEN)
   10 CONTINUE
C
C     PLOT THE NEXT COLUMN FROM BOTTOM UPWARDS
C
```

```
      J=J+1
      SX=SX+U
      DO 20 I=1,128
      SY=-FLOAT(129-I)*U
      AMP=REAL(CA(129-I,J))
      PHASE=AIMAG(CA(129-I,J))
      CALL PLCL(SX,SY,AMP,PHASE,U,PEN)
   20 CONTINUE
C
C     IF ALL COLUMNS HAVE BEEN PLOTTED STOP, OTHERWISE
C     CONTINUE WITH NEXT COLUMN.
C
      IF(J.LT.128)GO TO 9
      STOP
      END
C
C                    SOUBROUTINE PLCL
C
C     SUBROUTINE PLCL DECIDES WHICH TYPE OF APERTURE IS
C     REQUIRED FOR EACH CELL AND PLOTS IT.
C
      SOBROUTINE PLCL(SX,SY,AMP,PHASE,U,PEN)
C
C     IF AREA REQUIRED IS LESS THAN 1 PENSTROKE GO TO 10
C
      IF(AMP.LT.2.*PEN/U)GO TO 10
C
C     EVALUATE X1,X2,Y1,Y2 WHICH DETERMINE CORNERS OF
C     APERTURE
C
      Y1=SY+PEN
      Y2=SY+U
      DX=.5*U*AMP
      X1=SX+PHASE*U-.5*DX+PEN
      X2=SX+PHASE*U+.5*DX
C
C     DRAW THE OUTLINE FRAME OF THE APERTURE
C
      CALL PLOT(X1,Y1,3)
      CALL PLOT(X1,Y2,2)
      CALL PLOT(X2,Y2,2)
      CALL PLOT(X2,Y1,2)
      CALL PLOT(X1,Y1,2)
C
C     IF WIDTH OF APERTURE IS LT.OR.EQ. TO 2 PENSTROKES
C     THE PLOTTING IS COMPLETED. OTHERWISE FILL THE FRAME IN
C     WITH VERTICAL LINES SPACED 1 PENWIDTH APART, CHECKING
C     APTER EACH LINE IF PLOTTING IS COMPLELED.
C
    1 X1=X1+PEN
      IF(X1.GT.X2)X1=X2
      CALL PLOT(X1,Y1,2)
      CALL PLOT(X1,Y2,2)
      IF(X1.EQ.X2)GO TO 1000
```

```
      X1=X1+PEN
      IF(X1.GT.X2)X1=X2
      CALL PLOT(X1,Y2,2)
      CALL PLOT(X1,Y1,2)
      IF(X1.EQ.X2)GO TO 1000
      GO TO 1
C
C     THE POLLOWING STATEMENTS PLOT APERTURES WITH AREA
C     LESS THAN 1 PENSTROKE. FIRST CHECK IF AREA
C     REQUIRED IS LESS THAN THAT OF THE PENTIP, IF SO
C     NOTHING IS PLOTTED.  OTHERWISE DRAW A LINE OF THE LENGT
C     REQUIRED TO PLOT THE DESIRED AREA.
C
   10 PI=3.14159
      CH=.5*AMP*(U**2)-((PEN/2.)**2)*PI
      IF(CH.LT.0.)GO TO 1000
      DY=CH/PEN
      X1=SX+PHASE*U+PEN
      Y1=SY+PEN+(U-DY)/2.
      Y2=SY+PEN+(U+DY)/2.
      CALL PLOT(X1,Y1,3)
      CALL PLOT(X1,Y2,2)
 1000 RETURN
      END
```